LEBANESE AMERICAN UNIVERSITY

Novel Platinum II and Platinum IV Complexes Exhibit An Anti-Neoplastic Potential Against A549 Cancer Cell Line

By

Joy Baz

A thesis submitted in partial fulfillment of the requirements for the degree of Master of Science in Biological Sciences

School of Arts and Sciences

December 2021

LAU
الجامعة اللبنانية الأميركية
Lebanese American University

THESIS APPROVAL FORM

Student Name: Joy Baz I.D. #: 202000316

Thesis Title: Novel Platinum II and Platinum IV Complexes Exhibit An Anti-Neoplastic Potential Against A549 Cancer Cell Line

Program: Biology

Department: Natural Sciences

School: Arts and Sciences

The undersigned certify that they have examined the final electronic copy of this thesis and approved it in Partial Fulfillment of the requirements for the degree of:

Master of Science in the major of Biological Sciences

Thesis Advisor's Name: Dr. Costantine Daher

Signature: [redacted] Date: 22 / 12 / 2021
Day Month Year

Committee Member's Name: Dr. Christian Khalil

Signature: [redacted] Date: 22 / 12 / 2021
Day Month Year

Committee Member's Name: [redacted]

Signature: [redacted] Date: 22 / 12 / 2021
Day Month Year

LAU
الجامعة اللبنانية الأميركية
Lebanese American University

THESIS COPYRIGHT RELEASE FORM

LEBANESE AMERICAN UNIVERSITY NON-EXCLUSIVE DISTRIBUTION LICENSE

By signing and submitting this license, you (the author(s) or copyright owner) grants to Lebanese American University (LAU) the non-exclusive right to reproduce, translate (as defined below), and/or distribute your submission (including the abstract) worldwide in print and electronic format and in any medium, including but not limited to audio or video. You agree that LAU may, without changing the content, translate the submission to any medium or format for the purpose of preservation. You also agree that LAU may keep more than one copy of this submission for purposes of security, backup and preservation. You represent that the submission is your original work, and that you have the right to grant the rights contained in this license. You also represent that your submission does not, to the best of your knowledge, infringe upon anyone's copyright. If the submission contains material for which you do not hold copyright, you represent that you have obtained the unrestricted permission of the copyright owner to grant LAU the rights required by this license, and that such third-party owned material is clearly identified and acknowledged within the text or content of the submission. IF THE SUBMISSION IS BASED UPON WORK THAT HAS BEEN SPONSORED OR SUPPORTED BY AN AGENCY OR ORGANIZATION OTHER THAN LAU, YOU REPRESENT THAT YOU HAVE FULFILLED ANY RIGHT OF REVIEW OR OTHER OBLIGATIONS REQUIRED BY SUCH CONTRACT OR AGREEMENT. LAU will clearly identify your name(s) as the author(s) or owner(s) of the submission, and will not make any alteration, other than as allowed by this license, to your submission.

Name: Joy Baz

Signature: [redacted]

Date: 22 - 12 - 2021

LAU
الجامعة اللبنانية الأميركية
Lebanese American University

PLAGIARISM POLICY COMPLIANCE STATEMENT

I certify that:

- I have read and understood LAU's Plagiarism Policy.
- I understand that failure to comply with this Policy can lead to academic and disciplinary actions against me.
- This work is substantially my own, and to the extent that any part of this work is not my own I have indicated that by acknowledging its sources.

Name: Joy Baz

Signature: [redacted]

Date: 22 - 12 - 2021

Novel Platinum II and Platinum IV Complexes Exhibit An Anti-Neoplastic Potential Against A549 Cancer Cell Line

Joy Baz

ABSTRACT

Lung cancer is considered as the leading cause of cancer death and the second most diagnosed type of cancer. Although platinum-based chemotherapeutic drugs were relatively successful in treatment of lung cancer, patients frequently suffer from severe side effects, resistance and overall toxicity. This has lead scientists to invest in the discovery of novel platinum complexes that would improve efficacy and overcome toxicity. The present study aims to test the anti-neoplastic activity of novel Pt II and Pt IV complexes against A549 lung cancer cells and elucidate the mechanism of action involved. Cell cytotoxicity assay was conducted 72hrs post-treatment on A549 and mesenchymal stem cells using WST-1 kit. Cellular uptake of platinum complexes was studied by ICP-MS. Cell death analysis was studied using flow cytometry. Western blots were conducted to assess modulation of cell apoptotic markers. Free radical production was measured using reactive oxygen species kit. DNA degradation was evaluated by the comet assay. Results showed that Pt II and Pt IV complexes selectively reduce lung cancer cell viability. Cellular uptake results suggest a time-dependent active mode of transport for both complexes with Pt II being transported at higher rates and concentrations when compared to Pt IV. Flow cytometry revealed significant cell death by apoptosis and western blots showed the upregulation of intrinsic apoptotic markers.

Treatment with Pt II and Pt IV also showed significant amounts of free radical production and increased DNA damage. In conclusion, Pt II and Pt IV complexes induce lung cancer cell apoptosis through an intrinsic pathway and may be considered as promising selective and efficient anticancer drugs.

Key words: Lung cancer, Platinum complexes, Chemotherapy, Pt II, Pt IV, A549

TABLE OF CONTENTS

Chapter **Page**

LIST OF TABLES

LIST OF FIGURES

LIST OF ABBREVIATIONS

A549: Human Alveolar Adenocarcinoma Cells

APS: Ammonium persulfate

ATP: adenosine triphosphate

BAX: Bcl2 – Associated X Protein

Bcl2: B – Cell Lymphoma 2

BID: BH3 Interacting – Domain Death Agonist

BSA: Bovine serum albumin

c – PARP: Cleaved Poly (ADP – Ribose) Polymerase

CASP: Comet assay software package

CT Scan: Computed Tomography Scan

DMEM: Dulbecco's Modified Eagle's Medium

DNA: Deoxyribonucleic Acid

EtOH: Ethanol

FBS: Fetal bovine serum

HCl: Hydrochloric acid

HIV: Human Immunodeficiency Virus

HNO3: Nitric acid

IC_{50}: Inhibitory concentration 50

ICP-MS: Inductively coupled plasma mass spectrometry

KMnO4: Potassium permanganate

KMnO4: Potassium permanganate

MLKL: Mixed Lineage Kinase Domain-Like

MSC: Mesenchymal Stem Cells

NaCl: Sodium chloride

NaOH: Sodium hydroxide

NSCLC: Non-Small Cell Lung Cancer

PBS: Phosphate Buffered Saline

Pen/Strep: Penicillin-streptomycin

PET Scan: Positron Emission Tomography Scan

pH: potential hydrogen

Pt II: Platinum II – Based Complex (AK5)

Pt IV: Platinum IV – Based Complex (AK6)

Pt: Platinum

PVDF: Polyvinylidene fluoride

RIPK1: Receptor – Interacting Protein Kinase 1

RIPK3: Receptor – Interacting Protein Kinase 3

ROS: Reactive Oxygen Species

SBRT: Stereotactic Body Radiation Therapy

SCLC: Small-Cell Lung Cancer

SDS: Sodium dodecyl sulphate

SEM: Standard error of the mean

TBE: Electrophoresis buffer

TBS: Tris-buffered saline

TBS-T: Tris-buffered saline with Tween 20 xvi

TERT: Telomerase Reverse Transcriptase

TMI: Tail Moment Index

TNF: tumor necrosis factor

TNM: Tumor – Node – Metastasis System

UV: Ultraviolet

VEGF: Vascular Endothelial Growth Factors

WST: Water – Soluble Tetrazolium Salt

ZBP1: Z-DNA – Binding Protein 1

Chapter One

Literature Review

1.1. Cancer

1.1.1 Cancer Overview

Cancer is the uncontrolled growth of abnormal cells that can later on invade underlying tissue and eventually metastasize to distant sites of the human body; a group of these abnormal cells is known as the tumor (Cooper, et al., 2000). If tumor cells remain at their original site, the tumor is termed benign, however, when the tumor cells circulate via blood to reach other organ tissues in the body, the tumor becomes malignant (Cooper, et al., 2000). Cancer types and tumors are classified by their tissue of origin, and the most frequent type is carcinoma or adenocarcinoma which arise from the abnormal growth of epithelial cells (Cooper, et al., 2000). Some examples of carcinomas include cancer in the mouth, esophagus, stomach, colon, skin, breast and lung.

1.1.2. Normal Cell VS Cancer Cell

Normal cells rely on signals to replicate and divide in order to maintain homeostasis and balance in the human body, and since cancer is a disease of cell signaling, the cancer cells will hijack signaling pathways to inhibit or promote genes and proteins required for their abnormal survival and division. This will result in the disruption of the normal cell cycle and the emergence of immortal, abnormal and continuously dividing cancer cells (Fouad & Aanei, 2017).

If a normal cell acquires a gene mutation, it is then followed by repair mechanisms or cell death pathways to inhibit the inheritance and the effect of the mutation. Cancer cells tend to evade these repair and cell death mechanisms and accumulate mutations. Karyotypes done on cancer cells reveal a lot of genetic mutations including aneuploidy, deletions, insertions and translocations in a single cell (Sansregret & Swanton, 2017).

In addition, cancer cells are capable of rewiring normal metabolic processes to their benefit. For example, cancer cells are more metabolically active than normal cells and therefore require high amounts of glucose in order to survive. Therefore, cancer cells exploit pathways related to metabolism in order to produce enough nutrients for their abnormal growth and survival (Fouad & Aanei, 2017).

Similar to normal cells, tumors require nutrients and oxygen to grow and survive. For this reason, cancer cells hijack mechanisms responsible for the formation of new blood vessels also known as angiogenesis. Unlike normal cells, tumor cells will benefit from the direct blood circulation for migration and tissue invasion, rather than growth only (Hanahan & Weinberg, 2011).

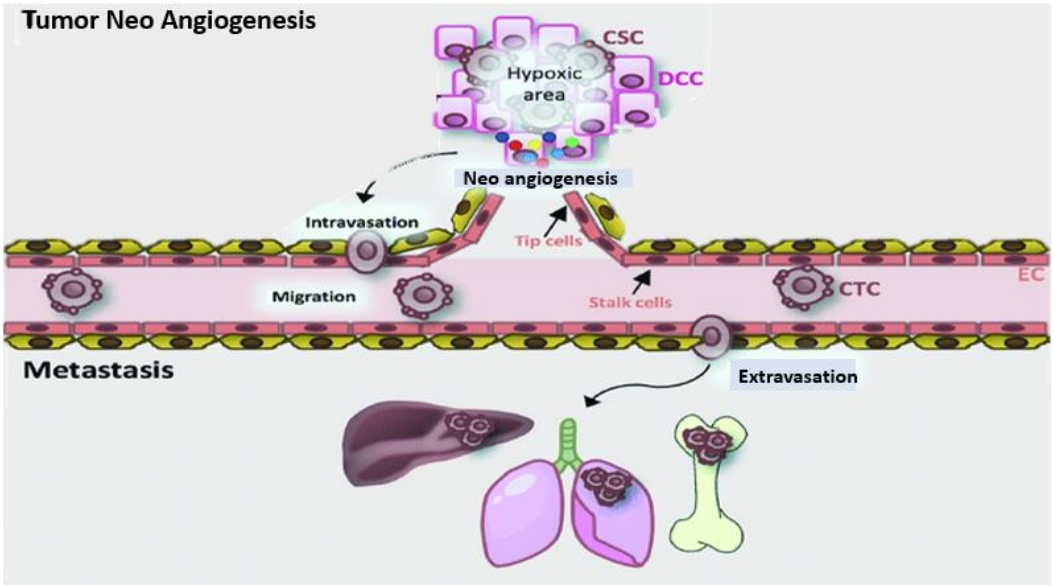

Figure 1.1: Angiogenesis in Cancer. This figure illustrates how tumor cells adapt to their hypoxic environment through angiogenesis in order to supply themselves with oxygen and other nutrients from the blood. The illustration demonstrates how cancer cells evade the blood vessel to metastasize into distant body organs (Turdo, et al., 2019). Modified from (Turdo, et al., 2019).

1.1.3. Tumor Development Stages

Many types of cancers develop at a specific age range, suggesting that cancer progression has several steps and requires the accumulation of mutations and abnormalities throughout many years (Cooper, et al., 2000). The deviation from a normal functioning tissue to becoming a fully malignant tumor is gradual and there are 5 steps leading to this transition: Hyperplasia, Metaplasia, Dysplasia, Macroscopic Growths and Malignant Carcinoma.

Hyperplasia is the first step in tumor development and it is when the tissue contains an increased mass of cells due to uncontrolled cellular division. Moreover, during this step, the cell morphology looks normal when examined under the microscope and the tumor is

still benign (Basu et al., 2018). Metaplasia is the second step of tumor development, and it is the transformation from a normal cell type in its normal location into a different, normal cell type but in an abnormal location (Cooper & McCathran, 2021). In lung cancer, smoke in the respiratory system causes metaplasia in certain tissues (Rigden et al., 2016). Dysplasia is the third step in tumor progression and it is when the cells begin to lose their normal features in which there is a change in nuclear and cytoplasmic morphology (Trivedi et al., 2016). During hyperplasia, metaplasia and dysplasia, the abnormal cells are still contained in the basement membrane and the tumor is still benign (Rivera et al., 2020). After these 3 stages, the abnormal features accumulate to form macroscopic growths that are highly hyperplastic and dysplastic like polyps, and these are also considered benign because they have not yet penetrated the basement membrane (Nijkang et al., 2019). Also, these macroscopic benign tumors grow to reach a certain size and then stop growing because they do not have access to oxygen and nutrients from the blood circulating in the stroma underneath. As soon as the tumor invades the basement membrane and stroma, the tumor becomes a malignant carcinoma and therefore can metastasize and spread to other organs through the circulatory system (Cooper, et al., 2000).

1.2. Lung Cancer

1.2.1. Lung Cancer Epidemiology

The most common cancers worldwide include lung cancer in addition to breast, prostate, colon and pancreatic cancer; however, lung cancer is the deadliest of them all and it accounts to around 30% of all cancer deaths worldwide, exceeding the deaths of the other common cancer types combined (Cooper, et al., 2000; Cruz, et al., 2011). Moreover, in

the United Sates, patients with a benign lung cancer tumor have a 5-year survival rate of around 60%, patients with mildly spread lung cancer have a 5-year survival rate of around 32% and it decreases in patients with completely metastasized lung cancer to reach 6%, knowing that most patients are diagnosed after lung cancer metastasis (Thandra, et al., 2021). Lung cancer is diagnosed in patients at an age range of 65-70 years old with a predominance in male gender (Thandra, et al., 2021). The genetic inheritance of mutations and genes associated with lung cancer increases the risk of getting the diseases by 1.7 folds (Thandra, et al., 2021).

1.2.2. Lung Cancer Types

The different types of lung cancer are grouped into 2 major categories that are named according to the morphological characteristic of the cancer cell: Small-Cell Lung Cancer (SCLC) and Non-Small Cell Lung Cancer (NSCLC) (Lemjabbar-Alaoui, et al., 2015). SCLC is less frequent than NSCLC, accounting to only 15% of total lung cancer cases while NSCLC accounts for the remaining 85% of lung cancers (Lemjabbar-Alaoui, et al., 2015). SCLC is derived from neuro-hormonal cells located in the lungs and it can develop due to exposure to air pollution and predisposition of genetic factors, however, the most contributing risk factor is smoking tobacco and pulmonary diseases that result from smoking (Lemjabbar-Alaoui, et al., 2015; Rudin, et al., 2021). Tumors in SCLC patients are located within the mediastinum and they are highly heterogeneous, meaning they contain multiple genetic mutations, and the most frequent mutation is the suppression of P53 gene which is linked to apoptosis and checkpoints in the cell cycle; once P53 is inactivated, the abnormal, mutated cells start to replicate indefinitely without being able to undergo programmed cell death and therefore will initiate tumorigenesis (Rudin, et al.,

2021). Because SCLC tumor cells are characterized by a very high replicating rate and an early metastatic capability, patients are almost never diagnosed with a benign tumor, instead, at diagnosis, the tumor cells have already broken through the basement membrane and metastasized to other vital organs like the brain and liver (Rudin, et al., 2021). NSCLC is the most prevalent lung cancer type and it is further subdivided into 3 major types: Adenocarcinoma, Squamous Cell Carcinoma and Large Cell Carcinoma (Zappa, et al., 2016). Adenocarcinoma is the most abundant type of NSCLC and lung cancer type in general, accounting up to 40% of total lung cancer patients (Siddiqui, et al., 2021). This type of NSCLC can develop in both tobacco smokers and nonsmokers, and unlike SCLC, adenocarcinoma tumor cells replicate at a slow rate and thus does not metastasize during early stages making it easier to diagnose and treat with a high progression – free survival rate (Lemjabbar-Alaoui, et al., 2015; Zappa, et al., 2016). Adenocarcinoma tumor cells arise from mucus-secreting alveoli in the lungs and it is usually found in lung periphery (Zappa, et al., 2016). Another NSCLC subtype is the squamous cell carcinoma which accounts to around 30% of lung cancer patients and it arises from squamous cells initially found in multiple areas of the respiratory tract including the lungs (Zappa, et al., 2016). The most common risk factor in this type of NSCLC is smoking (Siddiqui, et al., 2021). The last major NSCLC subtype is the large cell carcinoma and it accounts for 10% of all lung cancer patients, it is strongly liked to smoking and characterized by the presence of undifferentiated and immature cells most commonly in the center of the lugs (Zappa, et al., 2016; Siddiqui, et al., 2021).

1.2.3. Lung Cancer Risk Factors

Lung cancer has several risk factors. All these risk factors are not signs that the patient is determined to develop the lung cancer disease, however, they increase the risk of developing the disease. Age, gender, ethnicity and genetic factors like family history are some of the non-modifiable risk factors that affect lung cancer development; for example, genome – wide association studies have suggested that the inheritance of a certain locus on the telomerase reverse transcriptase, also known as TERT gene, would increase the risk of lung cancer diagnosis (Thandra, et al., 2021). Tobacco and marijuana smoking are modifiable risk factors commonly seen in lung cancer patients. When tobacco and marijuana are burnt, they produce multiple carcinogens that can enter the nucleus and damage DNA (deoxyribonucleic acid), resulting in mutations that will accumulate and increase lung cancer risk; this also applies for second-hand smokers (Thandra, et al., 2021). Also, several infections have been suggested to be linked with the development of lung cancer including Chlamydia pneumonia, Epstein – Barr Virus, HIV (Human Immunodeficiency Virus) and pulmonary tuberculosis (Cruz, et al., 2011; Thandra, et al., 2021). Environmental factors like arsenic in construction sites, radon gas, air pollution and radiation also contribute to lung cancer development (Cruz, et al., 2011; Thandra, et al., 2021).

1.2.4. Lung Cancer Stages

Grouping cancers according to types, mutations, tumor size and malignancy is beneficial for diagnosis, treatment options and helps in understanding the severity of the cancer disease in each individual patient (Lemjabbar-Alaoui, et al., 2015). There are 2 international systems used for cancer classification: Tumor – Node – Metastasis (TNM)

system and Number (I-IV) system. To use the TNM system, different cancer stages are denoted by T, N and M in which T describes the confined primary tumor size, N describes the spreading of tumor cells to local lymph nodes nearby, and M describes the spreading of tumor cells into distant sites and organs in the body and the formation of secondary tumors (Mirsadraee, et al., 2012). In addition, numbers are added to the T, N and M to describe levels of tumor size and spreading, for example, N1 means that the tumor spreads to 1-3 local nodes (Lemjabbar-Alaoui, et al., 2015). In the number system, stage 0 is indicative of the presence of abnormal cells confined in a certain area of a tissue, then the preceding stages: I, II and III indicate an increasing amount of tumor cells that are spreading into nearby lymph nodes and tissues. When the patient is diagnosed as stage IV, it indicates that the tumor is metastatic and has spread to distant organs in the patient and it is the most aggressive stage (Huang et al., 2020). Both the TNM system and the number system are used to group NSCLC patients at diagnosis (Lemjabbar-Alaoui, et al., 2015; Siddiqui, et al., 2021).

In SCLSC patients the TNM system can be used, however, the most common SCLC classification is simplified by using only 2 groups: limited stage and extensive stage. During the limited stage of SCLC, tumor cells are confined locally in a certain area, while during the extensive stage, tumor cells are undergoing metastasis and has spread to distant sites (Mirsadraee, et al., 2012).

1.2.5. Lung Cancer Diagnosis and Screening

The first clinical approach in patients with symptoms of lung cancer is performing a chest X-ray to look for any anatomically invading structures in the chest and lungs (Purandare & Rangarajan, 2015). This procedure does not confirm the presence or absence of cancer since in early lung cancer patients, tumors could be small in size to the point that it could not be detected with the x-ray radiograph (Latimer & Mott, 2015). Therefore, a Contrast-Enhanced Computed Tomography Scan (CT Scan) would be performed by subjecting the patient to x – rays beams that are capable of producing images on a computer of the different layers of the abnormal mass of cells previously located in the respiratory tract; however, before the procedure, contrast material like Iodine and Barium must be introduced into the patient body intravenously or via ingestion to improve the contrast and the quality of the cross-sectional images generated (Singh, et al., 2021; Latimer & Mott, 2015). This clinical procedure is frequently used in lung cancer diagnosis, but it has many side effects that could result due to radiation and contrast material (Singh, et al., 2021; Power, et al., 2016). Another approach is the Positron Emission Tomography (PET Scan) which is performed by the introduction of radioactive agents to detect elevations in cellular activity and metabolism which are characteristics of cancer cells (Purandare & Rangarajan, 2015). PET Scan can detect early – stage lung cancer in patients (Anand, et al., 2009). Invasive clinical tests and biopsies are normally performed on the patient to confirm the presence of cancer cells. The biopsies are then histologically tested to designate the stage of lung cancer and to detect the different mutations in the heterogeneous tumor in order to begin treatment. The type of biopsy extraction done mainly depends on the location of the tumor detected; for example, Bronchoscopy is an

invasive procedure that is applied when the tumor is detected in bronchi and it is done by inserting bronchoscope through the mouth into the lungs to visually examine the area and extract a tumor sample (Rudin, et al., 2021; Siddiqui, et al., 2021).

1.2.6. Lung Cancer Treatment

Treatment of lung cancer patients is very critical and depends on several factors including the type and stage of the lung cancer diagnosed, tumor heterogeneity and mutations along with the age of the patient. The treatment of NSCLC involves the use of surgery, chemotherapy, targeted therapeutics, radiotherapy and other combination therapies, however, the treatment of SCLC is limited to chemotherapy and radiotherapy due to rarity of cases and experiments done on SCLC patients (Siddiqui, et al., 2021). Surgery is the first option for stage I NSCLC patients and it has shown to greatly increase the percentage survival without the need of additional therapies and frequent hospital visits; moreover, it has fewer side effects than any other treatment (Zappa, et al., 2016). The surgery is of course done with the consent of the patient and depending on tumor size and location, some NSCLC surgeries include the cutting of part of the lung (Cafarotti, et al., 2020). SCLC patients are not recommended to treat the disease by surgical procedures since it is usually diagnosed when the tumor has already metastasized (Rudin, et al., 2021). Radiotherapy is another treatment recommended for lung cancer patients as a primary treatment or following surgery. This treatment option uses high-energy rays focused on the tumor cells to destroy the abnormal cells; however, this treatment itself can be cancer causative since the radiation emitted can cause mutations in normal cells (Hu, et al., 2019; Baskar et al., 2012). One common type of radiation therapy is **s**tereotactic body radiation therapy (SBRT) which is recommended for stage I and II of NSCLC and it works by

exposing very high radiation beams for a shorter treatment time (Zappa, et al., 2016; Baskar et al., 2012). Targeted therapy is also commonly used to treat cancer patients, however, eventually, the patient develops resistance towards the drug, making the tumor cells more aggressive and harder to treat (Lemjabbar-Alaoui, et al., 2015; Lu, et al., 2013). This type of treatment is based on the use of drugs that inhibit signaling pathways that are important for cancer cell survival and they work at best in combination to other treatments (Lemjabbar-Alaoui, et al., 2015). A lot of the complexes of these targeted therapeutics are Tyrosine Kinase Inhibitors like Bevacizumab that prevents angiogenesis by inhibiting Vascular Endothelial Growth Factors **(**VEGF); VEGF inhibitors are used to treat stage IV NSCLC (Garcia, et al., 2020; Lu, et al., 2013). Chemotherapy has been widely used to treat lung cancer, however, it is correlated with several harmful side effects on patients; the use of chemotherapeutic drugs in combination with other drugs have drastically decreased the side effects on patients and increased its responsiveness on cancer cells and solid tumors (Huang, et al., 2017). Platinum (Pt)-based complexes, like Cisplatin, are the most commonly used type of chemotherapeutic drugs for lung cancer treatment (Huang, et al., 2017).

1.3. Cell Death

There are several cell death mechanisms that can take place along the normal cell life cycle, and the activation of these mechanisms depend on distinct stimuli, cellular signals and protein availability (Elmore, et al., 2007). The organism uses cell death as one of several ways to remain organized and strictly regulated. For example, cell death is used during development for structural features, and it is also used throughout the individual life to get rid of cancerous and damaged cells (Alberts, et al., 2002). Cell death is of great

importance in cancer treatment and therapy because many cancer drugs developed are based on the manipulation of killer pathways that the cancer cell did not yet evade.

1.3.1. Apoptosis

Apoptosis is a known evolutionary conserved, sophisticated cell death machinery that gets rid of targeted cells by inducing cell shrinkage and nuclear fragmentation, leading to the complete abolishment of the apoptotic cell in a programmed and clean manner by phagocytosis (Xu, et al., 2019). Cell death in tumors has been highly associated with apoptosis which can occur via 3 main pathways, Intrinsic, Extrinsic and Perforin/Granzyme Pathways, depending on the signal transduction pathways activated within the cancer cell (Fulda, et al., 2006; Elmore, et al., 2007). The extrinsic pathway is triggered by the expression of specific death receptor ligands which are then recognized by complementary death receptors at the surface of the cancer cell (Fulda, et al., 2006). After the receptor-ligand interaction, the receptor aggregates leading to the recruitment of adapter proteins which will form a dimer and associate with the inactive pro-caspase 8 (Pfeffer, et al., 2018). Pro-caspase 8 can then activate itself by auto-cleavage, producing cleaved-caspase 8 which is the initiator caspase and a molecular marker of the extrinsic apoptotic pathway that can be detected by western blots (Pfeffer, et al., 2018). The activated caspase 8 will then initiate the execution pathway through the direct activation of apoptotic caspases downstream, like caspase 3, that will degrade intracellular proteins, or through BID (BH3 Interacting-Domain Death Agonist) activation which converges the extrinsic and intrinsic pathway at the level of the mitochondria, permeabilizing its membrane, activating caspase-3, leading to cell death (Pfeffer, et al., 2018; Xu, et al., 2019). The intrinsic pathway is triggered by several abnormal stimuli including stress,

DNA damage and oncogene overexpression (Elmore, et al., 2007). Unlike the extrinsic apoptotic pathway, the intrinsic pathway is not regulated by intracellular receptors, instead, it is regulated by a family of proteins called the Bcl-2 proteins which affect mitochondrial outer membrane permeability (Jan & Chaudhry, 2019). Bcl-2 proteins involved in apoptosis include the pro-apoptotic protein BAX and the anti – apoptotic protein Bcl-2, in which an increase in BAX expression will promote mitochondrial membrane permeabilization and the increase in Bcl-2 expression will prohibit mitochondrial membrane permeabilization; BAX expression is controlled by the tumor suppressor gene p53 (Fulda, et al., 2006). Therefore, p53 triggers the expression of BAX in high levels, BAX is then translocated into the membrane of the mitochondrion to permeabilize it and trigger the release of cytochrome c (Elmore, et al., 2007). Cytochrome c will then assemble with Apaf-1 and inactive procaspase 9 into an apoptosome to activate caspase 9 and start the execution pathway which, similarly in the extrinsic pathway, will activate downstream caspases like caspase 3 leading to cell death via apoptosis (Pfeffer & Singh, 2018). The perforin/granzyme pathway is an apoptotic pathway involved in the death of cancerous cells and it is induced by immune cytotoxic T cells which are equipped with granules containing granzymes and perforin molecules (Salti, et al., 2011). Upon cancer cell recognition, granzymes and perforin are released by exocytosis from the T cell and perforin molecules translocate into the membrane of the target cell to form a pore that allows for the diffusion of the granzymes into the cancer cell (Salti, et al., 2011). Granzyme B will trigger the activation of BID by cleavage which in turn induces the translocation of BAX into the outer membrane of the mitochondria, permeabilizing it, releasing cytochrome c, inducing apoptosome formation and caspase activation which

will result in cell death (Elmore, et al., 2007). Granzyme A is another granzyme involved in apoptotic cell death in which it is capable of regulating the expression of a tumor suppressor gene responsible for DNAse production which is responsible for DNA degradation of the targeted cancer cell (Elmore, et al., 2007).

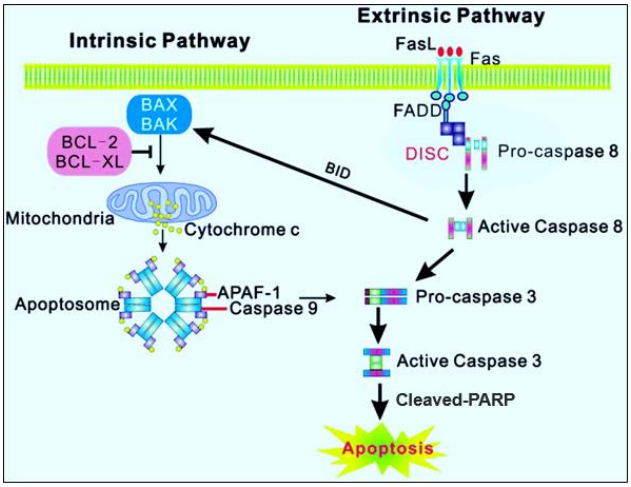

Figure 1.2: Apoptotic Cell Death Pathway. The figure schematizes the apoptotic pathway, namely the intrinsic and the extrinsic types. It also indicates how both pathways integrate each other at the end in the execution pathway to induce the programmed cell death of an abnormal cell (Tan et al., 2014). Modified from (Tan et al., 2014).

1.3.2. Necrosis

Necrosis is a type of cell death that is induced due to the accumulation of irreversible stresses and mutations in normal cells (Wallach & Kovalenko, 2014). Unlike apoptosis, this process is caspase-independent and it occurs in an unclean and unorganized manner in which the target cell swells and bursts to kill the cell and through doing that, it releases many cellular components like DNA and protein (Wallach & Kovalenko, 2014). Necrosis is highly associated with inflammation because the cellular components released during

bursting will recruit several pro-inflammatory molecules to the necrotic site (Khalid & Azimpouran, 2021).

1.3.3. Necroptosis

Necroptosis shares many characteristics with necrosis, like the swelling and rupture of the target cell, however, the distinct difference between the two forms of cell death is that necroptosis is a more controlled and regulated type of necrosis (Yu, et al., 2021). This process can occur through several identified and well distinct pathways which are sometimes linked to other forms of cell death, like apoptosis, due to the large pool of intracellular signaling proteins (Dhuriya & Sharma, 2018). One commonly identified pathway of necroptosis begins when TNF ligand binds to its complementary receptor TNFR and recruit RIPK1 (Receptor-Interacting Protein Kinase 1). RIPK1 then activates itself via phosphorylation, and recruits RIPK3 (Receptor-Interacting Protein Kinase 3), in order to assemble a complex called the necrosome. This necrosome can the bind and activate MLKL (Mixed Lineage Kinase Domain-Like) which becomes capable of translocating into the membrane of the target cell, permeabilizing it and resulting in its rupture (Dhuriya & Sharma, 2018). Other factors that involved in necroptosis pathways include reactive oxygen species (ROS) and Z-DNA-binding protein 1 (ZBP1) in breast cancer (Baik, et al., 2021; Gong, et al., 2019).

1.3.4. Reactive Oxygen Species

The presence of ROS in cells is damaging and oncogenic, however, many chemotherapy drugs induce cancer cell death by elevating ROS production to a certain threshold in the target cell (Yang, et al., 2018). These reactive oxygen species are capable of killing cancer

cells by hijacking signaling cascades of other cell death pathways including apoptosis and necroptosis. In apoptosis, ROS can permeabilize the outer membrane of the mitochondria and therefore induce cytochrome c release, form apoptosome and induce a caspase dependent death (Wang, et al., 2021). In necroptosis, ROS plays a role in the formation of the necrosome by RIPK1 and RIPK3 (Wang, et al., 2021). Also ROS over production by cancer treatments has shown to induce DNA damage in the target cell, leading to its death (Srinivas, et al., 2019).

1.3.5. Autophagy

Similar to apoptosis, autophagy is a conserved and programmed mechanism that leads to cell death. Autophagy occurs when an abnormal cell activates its own death through the use of organelles called lysosomes that contain digestive enzymes (Yun, et al., 2018). These lysosomes engulf and digest cellular components and organelles into products that are beneficial for the activity of other cells (Yun, et al., 2018). Beclin 1 is one of the genes involved in autophagy, and its expression in cancer cells has shown to interrupt the tumorigenesis process by killing cancer cells (Li, et al., 2020). Autophagy has been shown to play a promoting and a suppressing role in cancer progression, which makes this mechanism of death important to manipulate when synthesizing anti – cancerous drugs (Glick, et al., 2010)

1.3.6. Evasion of Cell Death

Cancer cells have the ability to accumulate mutations, replicate indefinitely and inherit their mutations due to their ability to evade cell death mechanisms; therefore, targeted therapeutics, chemotherapy and other types of treatments try to inhibit genes and proteins

that hijack cell death signaling cascades in order to initiate apoptosis, autophagy, ROS overproduction, necroptosis and necrosis. Cancer cells can evade necroptosis by avoiding necrosome formation through the ubiquitination of RIPK3 (Lim, et al., 2021). The cancer cell manipulates autophagy to promote cancer progression by triggering self-death in cancer cells that are under starvation stresses and in need of oxygen (Yun, et al., 2018). Also, autophagy promoting markers and proteins like Beclin-1 and ATG are shown to be down regulated in some cancer cells, meaning the cancer cell was capable of silencing death promoting genes to survive (Yun, et al., 2018). Tumor cells commonly evade the apoptotic pathway to survive and to become resistant over certain drugs and this is achieved by overexpressing pro-survival, anti-apoptotic Bcl-2 proteins and downregulation apoptotic markers like BAX; and this is seen in half of cancer types (Pfeffer & Singh, 2018).

1.4. Chemotherapy

Chemotherapy at first was an undesirable approach because of its aggressive effect on the patient body; however, after several studies and clinical applications, it has been shown to increase survival, improve cancer symptoms and facilitate the lifestyle of cancer patients, specifically in lung cancer patients (Rossi & Di Maio, 2016). Chemotherapeutics are currently used clinically and new complexes are still emerging in research and in the market with improved general toxicity and side effects.

1.4.1. Platinum-Based Chemotherapy

Platinum-based drugs are the most important chemotherapeutic and most promising approach in cancer treatment. Platinum drugs have been showing optimistic results in

lung cancer treatment; for example, the current standard approach for patients diagnosed with stage III and IV NSCLC is platinum-based chemotherapy and it increases patient survival (Rossi & Di Maio, 2016). The platinum compounds include the presence of platinum II or IV molecules. Platinum II complexes were the first to emerge, but platinum IV drugs are now considered promising because they conquer resistance and toxicity problems commonly caused by platinum II drugs (Zhong et al., 2020).

1.4.2. Commonly Used Platinum Drugs

Cisplatin is a common Pt II chemotherapeutic used for treatment of several cancers and it functions by binding to the nucleobases of DNA and triggering DNA damage, it also kills cancer cells by promoting apoptosis (Rossi & Di Maio, 2016). Cisplatin can also use other several damaging mechanisms including the overproduction of reactive oxygen species in cancer cells to trigger their death (Dasari & Tchounwou, 2014). There are 2 main disadvantages in the cisplatin treatments approach for cancer patients: resistance and side effects (Yimit, et al., 2019). After beginning cancer treatment with cisplatin, cancer cells evade the effects of the drug through several mechanisms including the blockage of copper transporter that allow platinum drug uptake into the cell, this will result in disease recurrence and the accumulation of additional mutations in the cancer cell (Yimit, et al., 2019; Dasari & Tchounwou, 2014). The side effects of cisplatin are known to be aggressive and they are the reason that many patients avoid chemotherapy (Yimit, et al., 2019). These side effects include damages in the nervous system and in the kidneys (Yimit, et al., 2019). Because cisplatin has shown to be an effective but toxic treatment, researchers have been focusing on creating new derivatives of cisplatin that are platinum – based, but less toxic. Carboplatin is one of the successful derivatives of

cisplatin, it has a similar DNA – binding mode of action, but it is less effective and induces fewer side effects. Unlike cisplatin, carboplatin is effective in only limited types of cancer including lung cancer (Dasari & Tchounwou, 2014). Both cisplatin and carboplatin are clinically used in the treatment of patients diagnosed with SCLC, and these chemotherapeutic agents work best in combination with other drugs (Dasari & Tchounwou, 2014).

1.4.3. Novel Pt II and Pt IV Complexes

The novel platinum complexes are Pt II and it Pt IV derivative. The Pt II adopts a square planar geometry and it is hydrophobic and small in size. The Pt IV adopts an octahedral geometry and two additional OH groups which render the complex hydrophilic and larger size (figure 1.3).

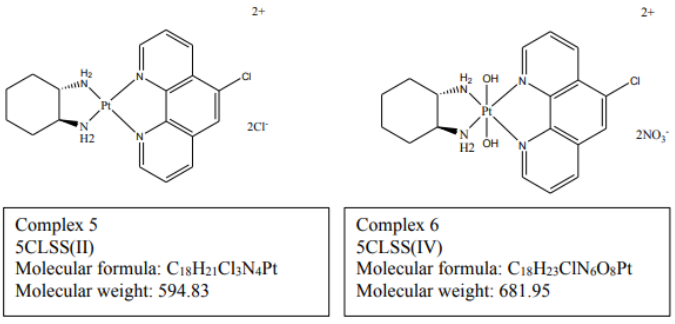

Complex 5
5CLSS(II)
Molecular formula: $C_{18}H_{21}Cl_3N_4Pt$
Molecular weight: 594.83

Complex 6
5CLSS(IV)
Molecular formula: $C_{18}H_{23}ClN_6O_8Pt$
Molecular weight: 681.95

Figure 1.3: The Structures of the Novel Pt II and Pt IV complexes. Pt II is complex 5 (left) and Pt IV is complex 6 (right).

1.5. Aim

Early-stage lung cancer patients are normally subjected to surgical resection of the tumor. Although, this procedure may cure some patients, a minority will remain recurrence-free at 5 years and most of the recurrences are located in distant sites (Hellmann, et al., 2014).

Such findings implicate that the incorporation of systemic therapies is of prime importance in order to improve the overall survival of the patients. Cisplatin-based systemic chemotherapy was shown to improve survival rate in advanced metastatic lung cancer (Qu, et al., 2019). Still, the currently available therapies could be more effective with much less side effects to patients. Therefore, there is a dire need for finding novel platinum-based chemotherapeutic drugs that help improving lung cancer treatment while reducing the commonly observed side effects. The aim of the present study is to test the chemotherapeutics activity of two novel platinum based complexes on NSCLC cell line A549 and elucidate the mechanism of action and uptake involved. The two complexes are platinum drugs, where AK5 is a platinum II complex and AK6 is its platinum IV.

Chapter Two

Material and Methods

2.1. Chemicals and Reagents

2.1.1. Cell Culture:

Product	Composition	Purchased from
DMEM	Dulbecco's Modified Eagle's Medium with 4.5 g/L glucose, L-glutamine, sodium bicarbonate and sodium pyruvate	Sigma Aldrich, Missouri, USA
PBS	Dulbecco's Phosphate Buffered Saline, 1X, with MgCl2 and CaCl2	Sigma Aldrich, Missouri, USA
Trypsin-EDTA	phenol red, 1X DMEM, PBS, & trypsin EDTA	Sigma Aldrich, Missouri, USA
Penicillin-Streptomycin	10K/10K stock 10,000 U/mL Pen/Strep	Gibco, Germany
Fetal Bovine Serum	heat inactivated, sterile and filtered.	Lonza, Germany

2.1.2. Cell Cytotoxicity Assay Kit:

CellTiter 96® Aqueous non-radioactive cell proliferation kit/ WST-1 (4-[3-(4-Iodophenyl)-2-(4-nitro-phenyl)-2H-5-tetrazolio]-1,3-benzene sulfonate)was purchased from Promega, USA.

2.1.3. Flow Cytometry Kit:

Annexin V-FITC apoptosis staining/detection kit was purchased from Abcam, Cambridge, USA.

2.1.4. Comet Assay Kit and Prepared/Purchased Solutions:

a. Kit (Trevigen, Maryland, USA) contains:

- **Lysis solution:** 40 ml Lysis Solution (catalog# 4250-050-01)
- **Alkaline Unwinding Solution:** pH>13 (200 mM NaOH, 1 mM EDTA): Per 50 ml of Alkaline Solution: 0.4 g NaOH Pellets, 250 µl 200 mM EDTA (catalog# 4250-050-04), 49.75 ml dH2O.
- **Alkaline Electrophoresis Solution:** pH >13 (200 mM NaOH, 1 mM EDTA): 8 g NaOH pellets, 2 ml 500 mM EDTA, pH=8, add to 1-liter dH2O (after NaOH is dissolved).
- **Fixation solution:** 10 µl 10X Fixation Additive (catalog# 4254-200-05), 30 µl dH2O, 50 µl methanol, 10 µl glacial acetic acid.
- **Staining solution:** 35 µl dH2O, 5 µl 20X Staining Reagent #1 (catalog# 4254-200-01), 5 µl 20X Staining Reagent #2 (catalog# 4254-200-02) 5 µl 20X Staining Reagent #3 (catalog# 4254-200-03). 50 µl 2X Staining Reagent #4.

b. **Stop solution:** 5% acetic acid solution (100 µl per sample area)

c. **NaOH and methanol:** purchased from Sigma Aldrich, Missouri, USA

d. **Acetic acid:** purchased from BDH, England

2.1.5. Western Blot

Triton X-100, Sodium dodecyl sulphate (SDS), glycine, methanol, polyoxyethylkene (20) sorbitan monolaurate (Tween 20) & bovine serum albumin (BSA) were purchased from Sigma Aldrich, Missouri, USA. Ammonium persulfate (APS) and Tris base were purchased from Fisher Scientific, USA. Laemmli buffer, TEMED, and Acrylamide/Bis solution were purchased from Bio- Rad, China. NaCl: purchased from HiMedia, India.

A. Solutions prepared:

RIPA buffer: 50 mM Tris-HCl, pH 8.0, 150 mM NaCl, 1% Nonidet P-40 (NP40) or 0.1% Triton X-100 0.5% sodium deoxycholate, 0.1% sodium dodecyl sulphate (SDS), 1 mM sodium orthovanadate.

Resolving gel (10%) (for 2 gels): 8 ml type II water, 6,6 ml 30 % acrylamide, 5ml buffer pH=8.8, 100 µL 20 % SDS, 200 µL 10 % APS,10 µL TEMED.

Stacking gel (10%) (for 2 gels): 4.2 ml type 2 water, 1.275 ml 30 % acrylamide, 1.875 ml buffer pH=6.8, 37.5 µL 10 % SDS, 75 µL 10 % APS, 7.5 µL TEMED.

Loading buffer (2x Laemmli buffer): 4% SDS, 10% 2-mercaptoethanol, 20% glycerol, 0.004% bromophenol blue, 0.125 M Tris-HCl

Buffer for separating gel (500 mL): 90.75 g Tris base, 500 mL distilled water, pH=6.8 .

Buffer for stacking gel (200 mL): 12 g Tris base, 200 mL distilled water, pH=8.8.

Running buffer 5X (1L): 15g Tris Base, 72g glycine, 25 mL 20% SDS, pH=8.3.

Transfer buffer 5X (500 mL): 7.6g Tris Base, 37.5g glycine, pH=8.5.

Transfer buffer 1X (100 mL): 20 mL Transfer buffer 5X, 60 mL distilled water, 20 mL methanol.

TBS 10X: 24.2 g Tris Base, 80 g Glycine, pH=7.6 .

Tris-buffered saline with Tween 20 (TBST) buffer: 40 mL TBS 10X, 360 mL distilled water, 0.1% Tween-20.

Blocking buffer: 5% bovine serum albumin (BSA) in TBST.

B. Antibodies:

Anti-β-actin: rabbit polyclonal, reactive with mouse, rat and human (Abcam, Cambridge, USA).

Anti-caspase 3: mouse monoclonal (Santa Cruz Biotechnology, CA, USA).

Anti-bcl2: rabbit polyclonal (Abcam, Cambridge, USA).

Anti-cytochrome c: rabbit monoclonal (Abcam, Cambridge, USA).

Anti-bax: rabbit polyclonal (Abcam, Cambridge, USA).

Anti-cleaved PARP-1: rabbit monoclonal (Abcam, Cambridge, USA).

Goat anti-mouse secondary antibody: HRP conjugate (Bio-Rad, Hercules, CA, USA).

Goat anti-rabbit secondary antibody: HRP conjugate (Bio-Rad, Hercules, CA, USA).

2.1.6. Cell line and Platinum complexes

- Platinum II and IV complexes were provided by professor Janice Aldrich-Wright from Western Sydney University. The molecular weights and the chemical formulas of the complexes are shown in figure 1.3.
- The A549 cell line, human alveolar adenocarcinoma was purchased from ATCC.

2.2. Methods

2.2.1. Cell Cytotoxicity Assay

The cytotoxicity assay was performed on the A549 cells and mesenchymal stem cells (MSCs). Cells were grown in Dulbecco's Modified Eagle's Medium (DMEM) at 37 °C with 5% CO2. Cells were plated in a 96-well plate at 10^4 cell/mL concentration. Cells were treated with the drugs at (150 μM concentration; 3- fold serial dilution) for 72 hours. Afterwards, the supernatants were thrown, 100μL and 10μL of WST-1 (4-[3-(4-Iodophenyl)-2-(4-nitro-phenyl)-2H-5-tetrazolio]-1,3-benzene sulfonate) were added to each of the 96 wells for 2 hours and incubated at 37 °C. Absorbances at 492nm was read using Labsystem Multiskan MS plate reader. The average of three experiments was used, samples run in triplicates.

2.2.2. Mesenchymal Stem Cell Isolation from Rat Bone Marrow

12-weeks old rats were provided by the animal facility at the Lebanese American University. The Animal Care and Use Committee (ACUC) of LAU gave the consent along with the Guide for the Care and Use of Laboratory Animals. Rats were killed done using CO2 overdose to provide a pain-free, and real fast death. Isolation of the femoral and tibial bones was accomplished using 70% ethanol and PBS. By a sterile

needle filled with DMEM, the bone marrows were flushed out into a 75 cm2 flask. Cells were placed in an incubator at 37 °C with 5% CO2 for 48 hours. Cells were then washed with 1% PBS and DMEM was often changed till confluency. The mesenchymal stem cells were spotted and recognized, under the inverted microscope (Nikon Eclipse TE300), by their spindle-shaped structure.

2.2.3. Pt II and Pt IV cellular uptake by ICP-MS

A final concentration of 10^6 A549 cell/mL were seeded in 6-well plates, and adhered overnight at 37°C in an environment of 5% CO2. The cells were then treated with a final concentration of 3 µM of either Pt II or Pt IV complexes. After 0, 1, 3, 6, 12 or 24 hours, the media was removed, and the cells were washed three times with cold PBS and left dry. The following day, 400uL of 68% HNO3 was added to each well, for an hour and a half, for complete digestion. The digests were moved to 15mL conical tubes, to which 7mL milliQ water was then added, followed by the addition of 7mL of internal standard of indium, which resulted in a final concentration of 2% HNO3. The cellular uptake of platinum was quantified via ICP-MS based on external standards. The results are averages of three different experiments (± SEM), optimized following the calibration curve and expressed as µM/cell.

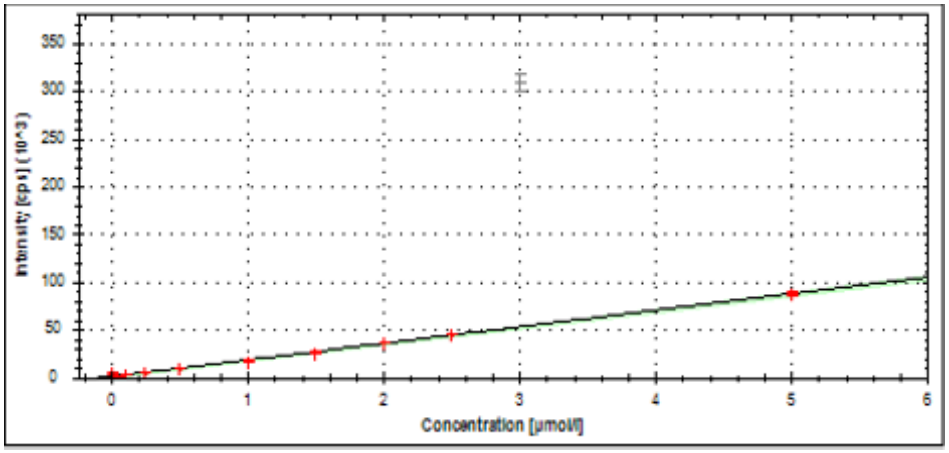

Figure 2.1: Calibration curve generated by plotting the peak areas (measured by the ICP-MS) against known concentrations. This curve was used to quantify the cellular uptake of both Pt II and Pt IV; $y= 1.7\times10^4 x + 0.86\times10^3$ and $R^2= 0.99788$

Table 2.1: Conditions and parameters selected on the ICP-MS machine. RF, radio frequwncy; He, helium; KED, kinetic energy discrimination

Parameter	Value
Plasma RF power	1550 W
Nebulizer gas flow rate	1.0 $L.min^{-1}$
Auxiliary gas flow rate	0.8 $L.min^{-1}$
Collision gas flow rate (He)	4.7 $L.min^{-1}$
KED voltage	3 V
Extraction lens	-250 V
Isotope monitored	^{194}Pt
Dwell times	10 ms

2.2.4. Flow Cytometry

Annexin V-Phycoeryhtrin (Annexin V-PE) and 7-AAD (7-amino-actinomycin D) staining (Guava Nexin Reagent Kit, Luminex, Austin, Texas, U.S.A), were used to analyse cell death and the path of death it takes 24, 48 and 72hrs post-treatment. A549 cells were seeded in a 6-well plate (10^5 cells/mL) and treated with 4x IC_{50} concentration of Pt II and Pt IV. Plates were incubated at 37 °C and 5% CO2. After 24, 48 and 72 hours, supernatant/medium was moved from each well into respectively labelled conical

tubes onto ice. The cells were trypsinized with 200µL trypsin /well, and the detached cells were moved on top of the previously collected media respectively /labelled conical tube. Then, 10uL of this mix was added to 10uL Trypan blue to count the cells under the inverted microscope (Nikon Eclipse TE300). A final concentration of 500 cells/uL was obtained and adjusted per condition into Eppendorf tubes on which, centrifugation at 1500 rpm for 5 minutes at 4°C, was performed. The supernatant was dissolved, and the pellet was suspended in 100 µL Guava Nexin Reagent buffer, provided by the kit. Each sample was pipetted onto a 96-well plate, and incubated in the dark for 10 minutes. Cells were then analyzed using the Guava® easyCyte 8HT Benchtop Flow Cytometer (Millipore, Luminex, USA). AnnexinV/7- AAD data was measured on FL1-H versus FL2-H scatter plot.

2.2.5. Western Blot

6-well plates were used to seed A549 cells. Cells were incubated overnight at 37°C with 5% CO2. Following the incubation, cells were treated for 72 hours with 4x IC_{50} concentration of each the Pt II, and the Pt IV drugs. At 72 hours, the 6-well plates were placed on ice, and cells were removed and placed in 15mL conical tubes. Tubes were centrifuged at 1500 rpm for 5 minutes at 4 °C. The supernatant was discarded, and the pellet was kept on ice inside the tubes. On the wells, 200 uL of lysis RIPA buffer were added, and the extra cells were removed using a scrapper. The removed cells were added over the pellet, and the conical tubes were placed on the shaker for 10 minutes on ice to allow the pellet and the cells to be mixed. The mixed solution was then centrifuged at 13000 rpm for 15 minutes at 4 °C to take the supernatant. The supernatant, which contains the protein lysate, from each sample was placed in the

labeled Eppendorf tube. Using a 96-well plate and the Bio-Rad protein assay (Bio-Rad, Hercules, CA, USA), 2 μL of the protein lysate was placed with 3 μL RIPA buffer and 200 μL of diluted Bradford reagent. This was done for each sample. The samples in the plate were allowed to run in the VarioskanTM LUX Multimode microplate reader (ThermoFisher) to read the absorbance at 595nm. The results that came out from the reader was utilized to make the samples for the loading the gel; 20 μg of each protein condition in RIPA buffer and 2x Laemli Buffer containing 9% β-mercaptoethanol. Once the samples were prepared, they were heated at 100°C for 5 minutes. Protein samples were heated at 100°C for 5 minutes prior to loading. Equal volumes (15 or 20 µl) were loaded to 10% SDSPAGE. The voltage was set at 90 V for 30 minutes, then at 120 V for 90 minutes. In the meantime, PVDF membranes and filter pads were cut, soaked in methanol followed by water, then left in transfer buffer. Once the run was over, gels were transferred to PVDF membrane (Pall Corporation, Ann Arbor, USA) and blocked with blocking buffer (1× TBS, 0.1% Tween-20, 5% skim milk) for 1 hour. The membranes were then probed with primary antibodies against several apoptotic and antiapoptotic proteins at 4°C overnight. Membranes were then washed thrice for 5 minutes with TBST in order to remove the primary antibodies, treated with secondary antibodies for 90 minutes, and washed thrice for 10 minutes with TBST afterwards. Detection of proteins was performed using the chemiluminescence ECL kit (Bio-Rad, U.S.A). 500 µl of peroxide solution were mixed with 500 µl of luminol/enhancer solution and spread all over the membrane. The membrane was then left in dark for five minutes before imaging. Blot images were finally obtained with the ChemiDoc MP imaging system (Bio-Rad, U.S.A).

2.2.6. Comet Assay for Analysis of DNA Damage by Pt II and Pt IV on A549

Comet Assay kit (4251-050-k) purchased from R&D systems (Minneapolis, USA) was used. A concentration of 10^5 A549 cells/ml was plated in 6-well plates. Treatment with Pt II and Pt IV was done 24 hours after plating. Cells were incubated at 37°C and 5% CO2. 72 hours after treatment, KMnO4 was placed over one of the wells to generate the positive control, and PBS was added over another well to generate the negative control and kept for 25 minutes. In the meantime, cells were collected in 15mL conical tubes, and were washed with PBS and then trypsinized with 200 μL of trypsin for 5 minutes. Cells were collected and added over the conical tubes. The same procedure was repeated on the positive and negative controls. The whole solution of cells was centrifuged at 3000rpm for 10 minutes. Supernatant was thrown away, and the pellet was suspended in PBS to collect 105 cells/ml. The needed concentration of cells was placed in Eppendorf tubes with low melting agarose (LMA) at 37°C at a ratio of 1:10. The solution of LMA was spread on the whole surface of the comet slide for each condition. Slides with the LMA solution kept in the dark at 4°C for 30 minutes. Once the agarose solidified, the slides were placed in the Comet Assay lysis solution at 4°C overnight. The next day, the lysis solution was removed, and the slides were immersed in an alkaline unwinding solution (200mM EDTA, 1mM NaOH) in the dark and at room temperature for 30 minutes. The slides were washed with an alkaline electrophoresis buffer solution buffer (1X TBE, pH 13) for 5 minutes, placed on the electrophoresis apparatus, and covered with Electrophoresis buffer (1X TBE, pH 13) for 40 minutes at 20V. At the end of the electrophoresis, the slides were washed twice with

type II water for 5 minutes, and then with 70% ethanol for 5 minutes. To fixate the samples on the slide, they were immersed in a fixation solution for 20minutes, and then with type II water for 30 minutes. Slides were paced in a staining solution for around 30 to 40 minutes at room temperature until the comet tails were observed well under the microscope. The reaction was stopped after the observation of the comet tails with 5% acetic acid (100uL) for 15 minutes. Slides were washed from the acetic acid and were allowed to try to be stored in the dark for later analysis. For each condition on the slides, 50 cells were selected and assessed based in the intensity the tail using the Comet Analysis Software Package (CASP). The damage of the DNA is assessed based on the tail moment index (TMI) which is equal to the multiplication of the tail DNA content of cells by the tail length and divided by 1000.

2.2.7. Reactive Oxygen Species Production

To detect the production of reactive oxygen species by the platinum complexes, the ROS Assay Kit (Abcam, Cambridge, USA) was utilized. A549 cells were plated into 96-well plates at 25000 cells/mL using phenol red media. After 24 hours, cells were washed twice with PBS and stained with DCFDA of 25 μM concentration. DCFDA was kept on the cells for 45 minutes in the dark and then removed and 100 μL of phenol red free media was added over the wells. 50 μL of Pt II and Pt IV were added to the platted cells at a concentration of 4x IC_{50}. At 72 hours after treatment, the plate was scanned using the VarioskanTM LUX Multimode microplate reader (Thermo Fisher) to measure the fluorescence at an excitation/emission of 485/535 nm.

2.2.8. Statistical Analysis

Results were reported as mean ± SEM from three different trials. They were analyzed by one-way ANOVA. Statistical difference between groups was analyzed via independent statistical Student T-test and was considered significant when $p<0.05$ (Tukey's multiple comparisons test).

Chapter Three

Results

3.1. Cytotoxicity of Pt II and Pt IV Complexes Against A549 Cells

To test the cytotoxicity of the platinum complexes on cells, the colorimetric reagent WST-1 (water-soluble tetrazolium salt) was used. When the cancer cell A549 is viable, it is metabolically active and therefore releases enzymes into the cell culture medium, including the enzyme cellular mitochondrial dehydrogenase. Therefore, in the cell cytotoxicity assay, if the plate-well contains viable cells it will produce cellular mitochondrial dehydrogenase that will convert tetrazolium salts added into formazan. The amount of formazan can be then measured in terms of absorbance at 440nm (Scarcello et al., 2020). After analysis of the results, the assay will provide us with an IC_{50} which is a universal measure that denotes the potency of the drug and the concentration required to kill half of the cells that are treated (Aykul & Martinez-Hackert, 2016).

When the A549 cells where treated with different concentrations of the Pt II and Pt IV complexes, the results showed that both drugs were toxic on the cancer cells and resulted in their death, however each with a specific IC_{50} (figure 3.1). The Pt II drug, also known as AK5, had an IC_{50} of 0.239 µM and the Pt IV drug, also known as AK6, had an IC_{50} of 1.445 µM (table 3.1).

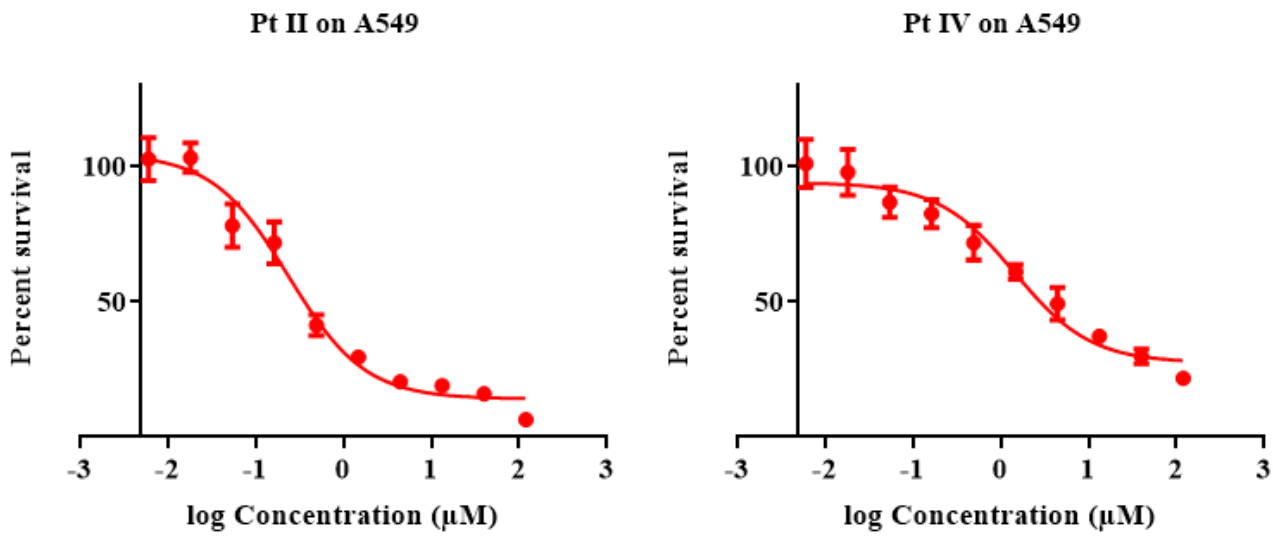

Figure 3.1: The cytotoxic effect of Pt II and Pt IV on the survival of A549 cells. The cells where treated with different concentrations of the complexes and analyzed 72hrs post-treatment. Data point denote mean ± SEM. n = 3 from three independent experiments where samples were run in triplicates.

Table 3.1: IC_{50} values of the Pt II and Pt IV complexes calculated after the cytotoxicity assay on A549 cells.

Drug	**Cell Line**	**IC_{50} (µM) ± SEM**
Pt II (AK5)	A549	0.239 ± 0.006
Pt IV (AK6)	A549	1.445± 1.02

3.2. Cytotoxicity of Pt II and Pt IV Complexes Against MSC Cells

MSCs were also treated with different concentrations of the Pt II and Pt IV complexes for 72hrs. Results showed that both complexes were not toxic on the tested normal cells (figure 3.2). Both, the Pt II drug and the Pt IV drug had extremely high IC_{50} values of 17021 µM and 16779 µM respectively.

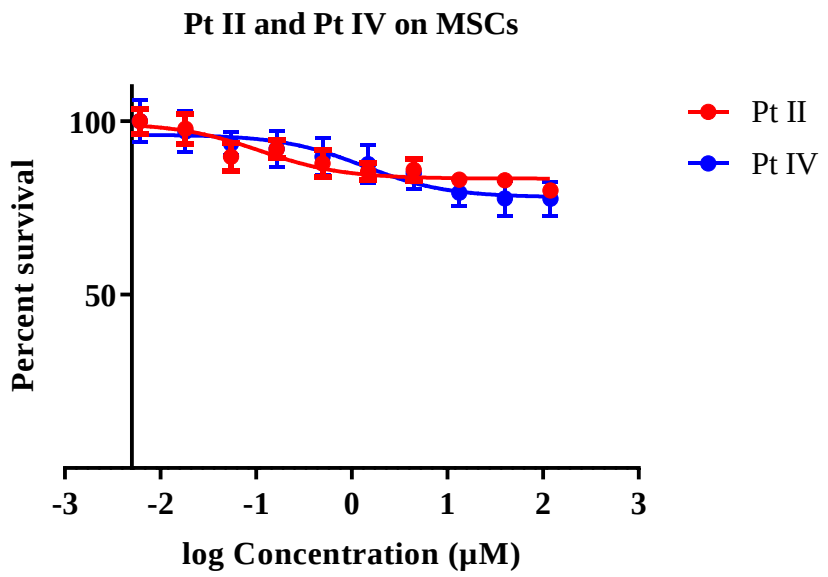

Figure 3.2: The cytotoxic effect of Pt II and Pt IV on the survival of MSCs. The cells where treated with different concentrations of the complexes and analyzed 72hrs post-treatment. Data point denote mean ± SEM. n = 3 from three independent experiments where samples were run in triplicates.

3.3. Cellular uptake of Pt II and Pt IV complexes in A549 cancer cells

The A549 cells were treated with either Pt II or Pt IV complexes at a final concentration of 3 µM. After 1, 3, 6, 12, 24 or 30 hrs, cellular uptake of each complex was quantified by ICP-MS based on external standards. Results showed high intracellular/extracellular ratios in both Pt II and Pt IV complexes, which indicates that the drugs were being actively uptaken into the cells (figure 2.3). According to the results, Pt II complex uptake in A549 cells was faster when compared to the Pt IV complex (figure 3.3, table 3.2). Also, Pt II exhibited higher uptake than Pt IV at 30hrs post treatment (figure 3.3, table 3.2). It is also important to note that the uptake of the complexes was time-dependent. Pt II uptake showed a plateau at 24 hr but Pt IV uptake kept increasing after 30hrs post-treatment (figure 3.3, table 3.2).

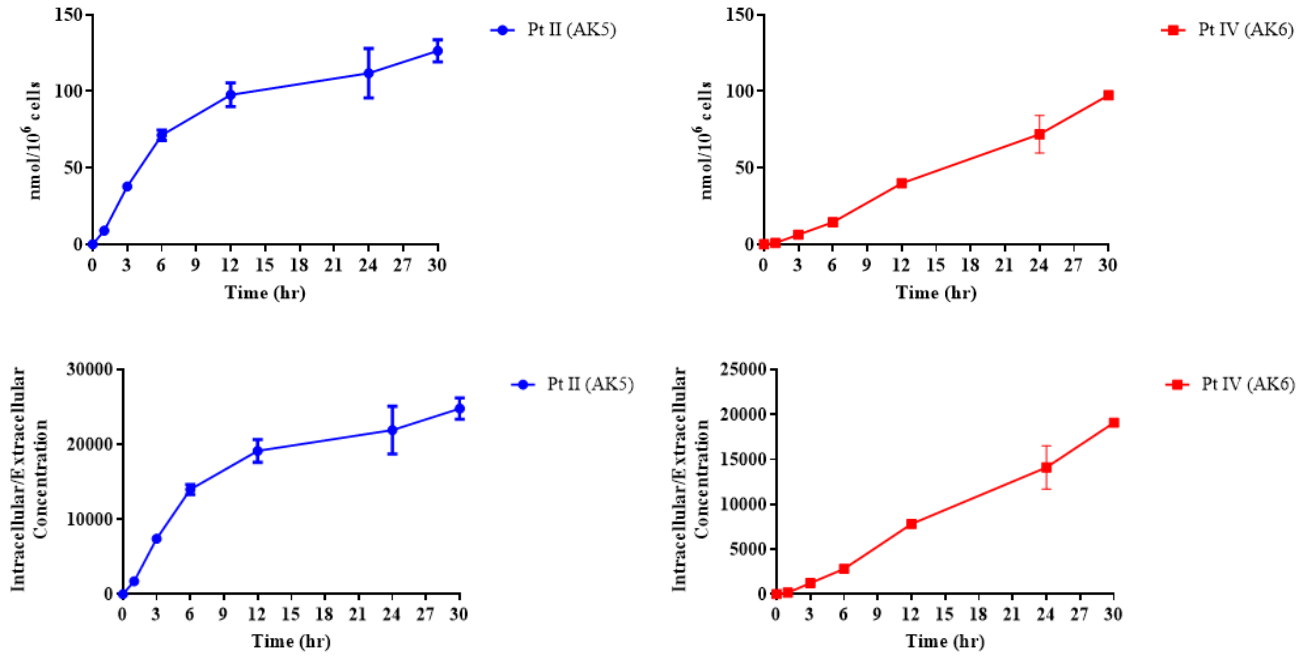

Figure 3.3: ICP-MS analysis of the uptake of Pt II and Pt IV complexes by A549 cells. Graphs reveal cellular concentration in nmol/10^6 cells (top) and the ratio of intracellular concentration to extracellular concentrations (bottom) for each complex. Data points denote mean ± SEM. n = 3 from three independent experiments where samples were run in triplicates.

Table 3.2: Cellular uptake of Pt II and Pt IV complexes by A549 cells. Table reveals the average value of cellular concentration in nmol/10^6 cells (top) and the ratio of intracellular concentration to extracellular concentrations (bottom) for each complex. Data points denote mean ± SEM. n = 3 from three independent experiments where samples were run in triplicates.

Time in hours (hr)	Complex	1hr	3hr	6hr	12hr	24hr	30hr
Average Cellular Concentration (nmol/10^6 cells)	Pt II (AK5)	8.924767 ± 0.89	37.85273 ± 2.86	71.3013 ± 3.42	97.6255 ± 7.77	111.7585 ± 16.22	126.4242 ± 7.28
Average Cellular Concentration (nmol/10^6 cells)	Pt IV (AK6)	0.906733 ± 0.69	6.340833 ± 1.37	14.4347 ± 0.77	39.88973 ± 2.09	71.96887 ± 12.23	97.3763 ± 0.58
Average Concentration Ratio (intracellular/extracellular)	Pt II (AK5)	1749.954 ± 170.26	7422.105 ± 559.95	13980.65 ± 671.53	19142.25 ± 1523.35	21913.43 ± 3180.79	24789.06 ± 1428.32
Average Concentration Ratio (intracellular/extracellular)	Pt IV (AK6)	177.7908 ± 136.02	1243.301 ± 269.23	2830.333 ± 151.25	7821.516 ± 409.86	14111.54 ± 2395.97	19093.39 ± 113.67

3.4. Cell Death Analysis of Pt II and Pt IV complexes in A549 cancer cells by flow cytometry

Annexin V/7AAD staining was used on A549 cells treated with 4x IC_{50} concentrations of Pt II and Pt IV for 24, 48 and 72hrs. Cisplatin was used as a positive control. At 24hrs post-treatment, results reveal that both complexes significantly induced A549 cell death by apoptosis when compared to the control ($P<0.0001$ and $P<0.001$) (figure 3.4, figure 3.7). There is no significant difference in cell death by necrosis at 24hrs among the various groups (figure 3.7). At 48 and 72hrs post-treatment, both Pt II and Pt IV complexes caused significant increases ($P<0.01$ and $P<0.05$) in the percentages of apoptotic and necrotic A549 cells compared with the control (figure 3.8, figure 3.9).

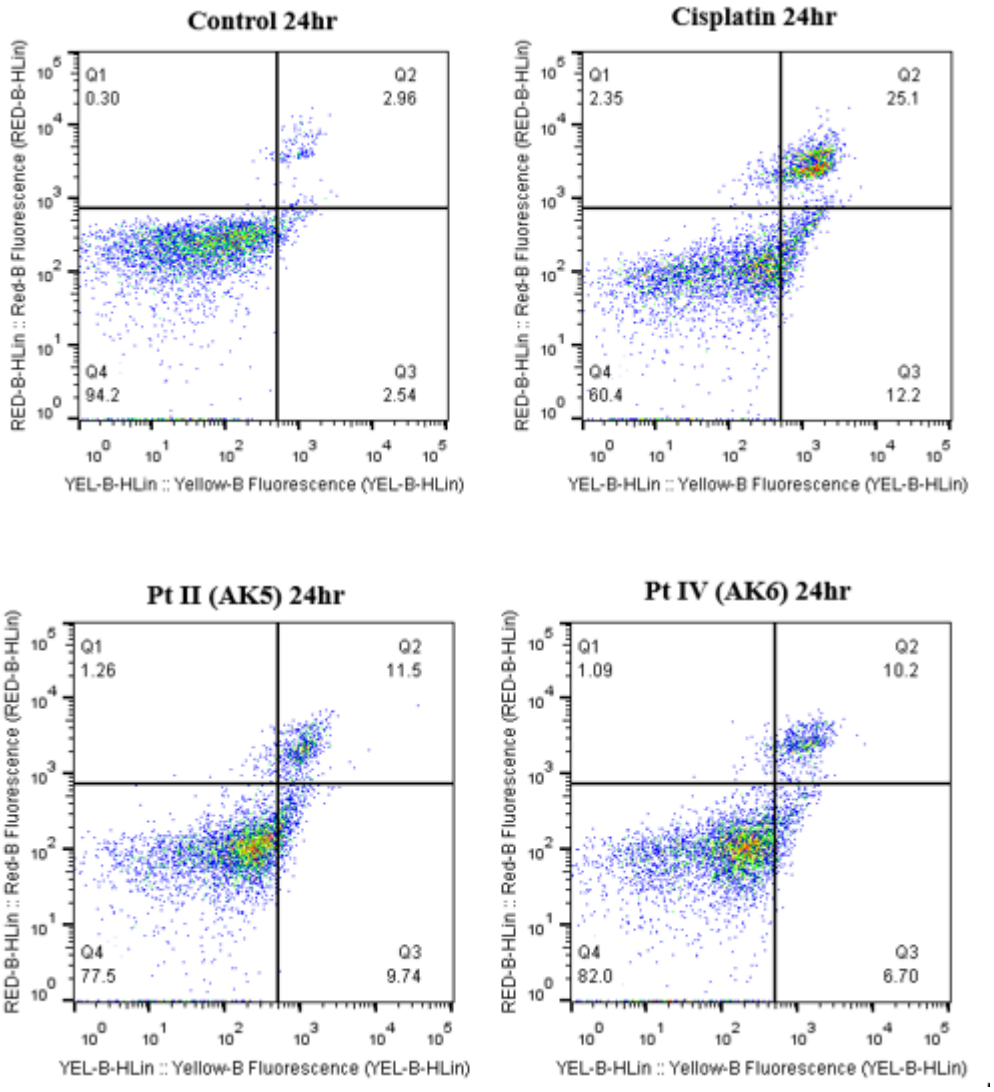

Figure 3.4: Cell death analysis by flow cytometry of A549 cells 24hrs post-treatment. Graphs reveal early, late and necrotic cell death after 24hrs in control and cells treated with Cisplatin, Pt II and Pt IV complexes using 4x IC_{50} concentration. Data points denote mean ± SEM. n = 3 from three independent experiments where samples were run in triplicates.

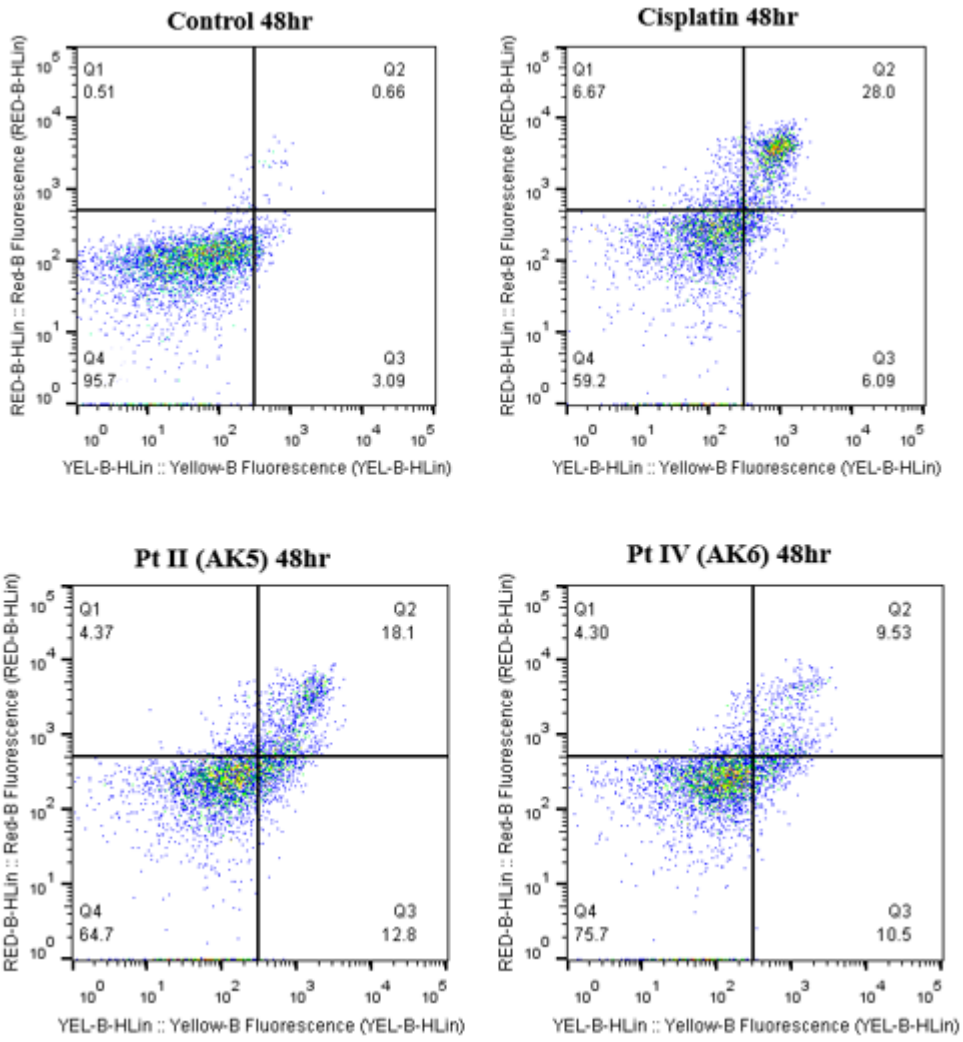

Figure 3.5: Cell death analysis by flow cytometry of A549 cells 48hrs post-treatment. Graphs reveal early, late and necrotic cell death after 48hrs in control and cells treated with Cisplatin, Pt II and Pt IV complexes using 4x IC_{50} concentration. Data points denote mean ± SEM. n = 3 from three independent experiments where samples were run in triplicates.

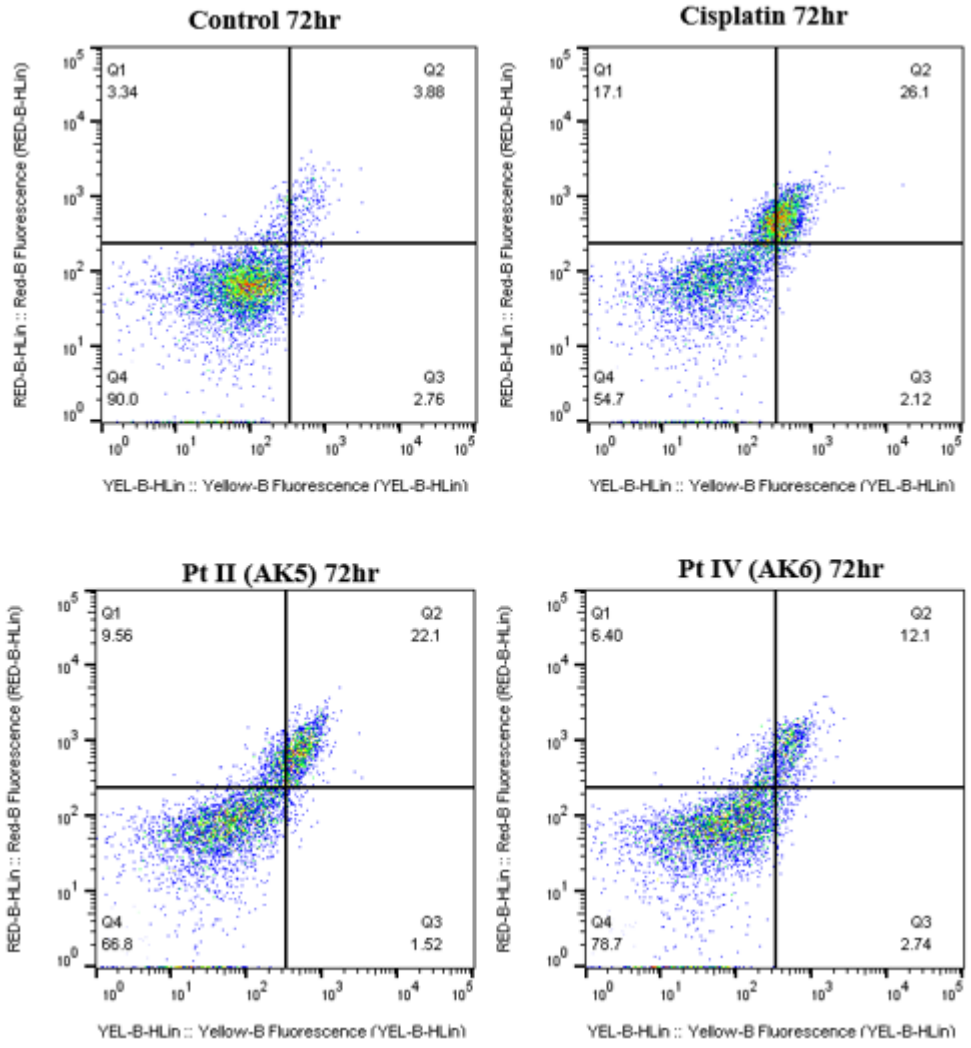

Figure 3.6: Cell death analysis by flow cytometry of A549 cells 72hrs post-treatment. Graphs reveal early, late and necrotic cell death after 72hrs in control and cells treated with Cisplatin, Pt II and Pt IV complexes using 4x IC_{50} concentration. Data points denote mean ± SEM. n = 3 from three independent experiments where samples were run in triplicates.

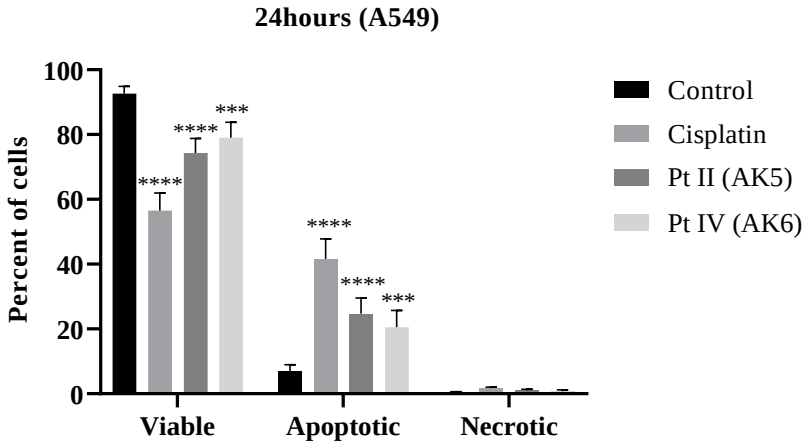

Figure 3.7: Bar graph representing percent viable, apoptotic and necrotic cells at 24hrs. **** indicates P<0.0001 compared with the control. *** indicates P<0.001 compared with the control (measured by one-way ANOVA). Data points denote mean ± SEM. n = 3 from three independent experiments where samples were run in duplicates.

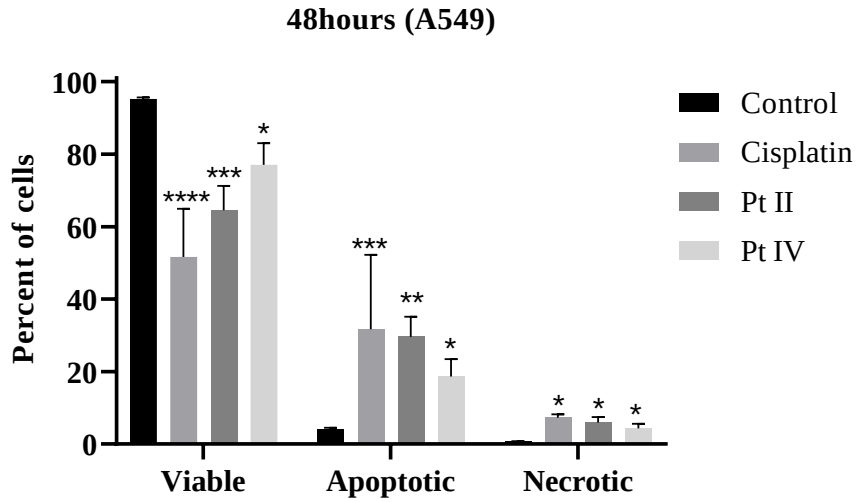

Figure 3.8: Bar graph representing percent viable, apoptotic and necrotic cells at 48hrs. **** indicates P<0.0001 compared with the control. *** indicates P<0.001 compared with the control. ** indicates P<0.01 compared with the control. * indicates P<0.05 compared with the control (measured by one-way ANOVA). Data points denote mean ± SEM. n = 3 from three independent experiments where samples were run in duplicates.

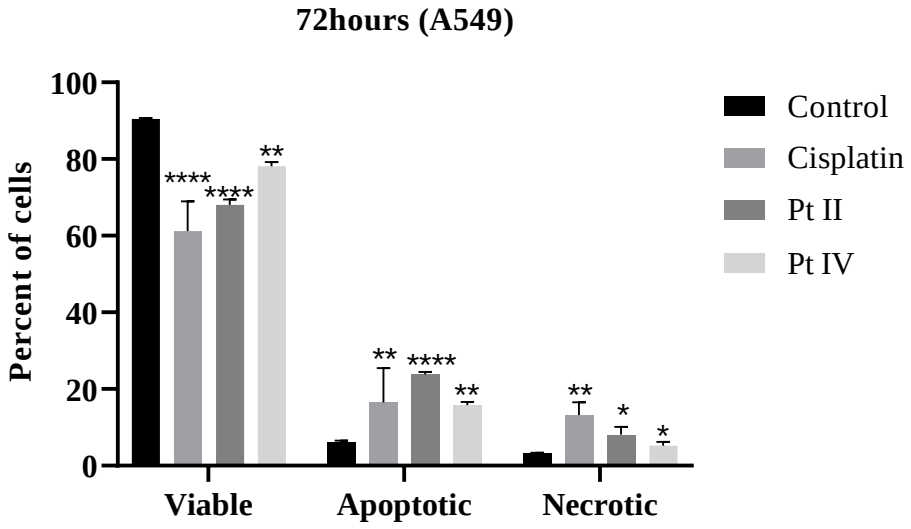

Figure 3.9: Bar graph representing percent viable, apoptotic and necrotic cells at 72hrs. **** indicates P<0.0001 compared with the control. ** indicates P<0.01 compared with the control. * indicates P<0.05 compared with the control (measured by one-way ANOVA). Data points denote mean ± SEM. n = 3 from three independent experiments where samples were run in duplicates.

3.5. Reactive Oxygen Species (ROS) Production

To measure ROS production upon treatment with 4x IC_{50} of the Pt II and Pt IVcomplexes, the treated cells where stained with DCFDA which proportionally increases with ROS detection and it is measured by the amount of fluorescent products produced when a blue led light is activated. TBHP was used as a positive control. Results indicate that both complexes produce significant amounts of ROS in A549 cells 72hrs post-treatment (P<0.0001 and p<0.001) compared to untreated, control cells. ROS production in Pt IV (AK6) treated cells is higher than the in Pt II (AK5) treated cells (figure 3.10).

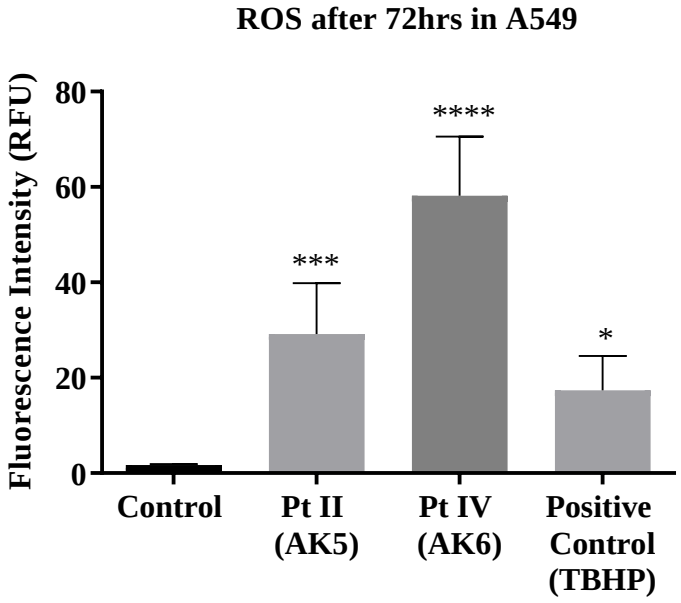

Figure 3.10: Bar graph representing ROS production 72hrs post-treatment with Pt II and Pt IV on A549 cells. **** indicates P<0.0001 compared with the control. *** indicates P<0.001 compared with the control. * indicates P<0.05 compared with the control (measured by one-way ANOVA). Data points denote mean ± SEM. n = 3 from three independent experiments where samples were run in triplicates.

3.6.Western Blots

Western blots were done to measure the protein levels of apoptotic markers in A549 cells 72hrs post-treatment with 4x the IC_{50} of Pt II and Pt IV complexes. All results were normalized over β-Actin. Results were presented as bands visualized by the ChemiDoc imaging system, quantified using ImageLab and presented as bar graphs using GraphPad Prism. n =3 from three independent experiments. The protein levels of cleaved PARP, BAX/Bcl_2 ratio, cleaved caspase 3 and cytochrome c were shown to be significantly upregulated, confirming the induction of intrinsic apoptosis via Pt II and Pt IV.

3.6.1. Cleaved Poly (ADP-Ribose) Polymerase: Cleaved-PARP-1

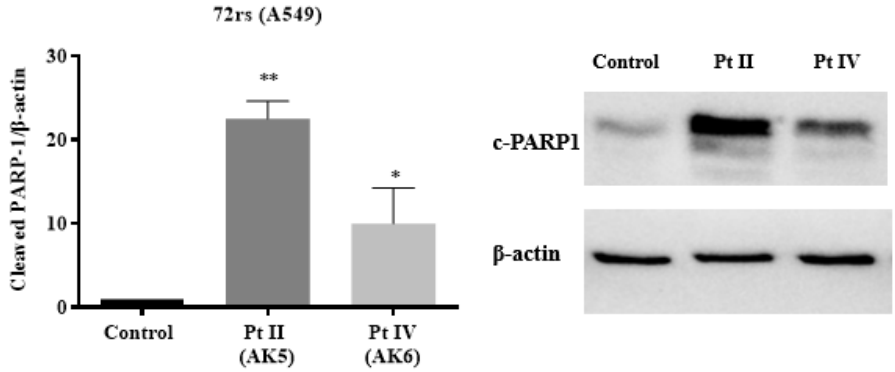

Figure 3.11: Bar graph and western blot images of cleaved-PARP-1 and β-actin 72hr post-treatment with Pt II and Pt IV on A549 cells. ** indicates P<0.01 compared with the control. * indicates P<0.05 compared with the control (measured by one-way ANOVA). Data points denote mean ± SEM. n = 3 from three independent experiments.

3.6.2. Bcl2 – Associated X Protein (BAX)

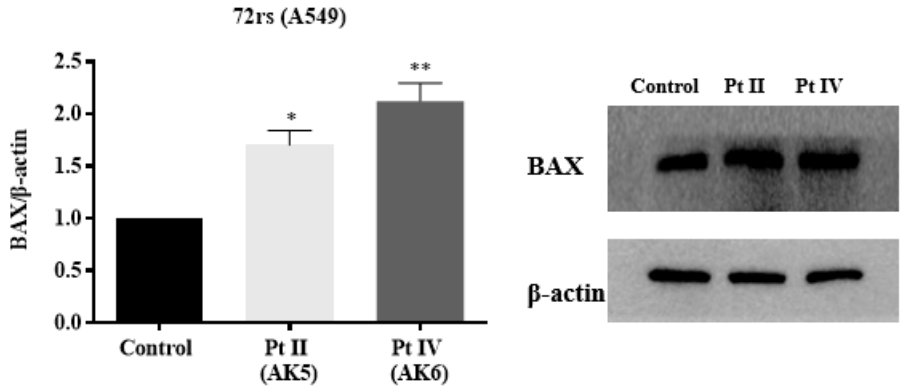

Figure 3.12: Bar graph and western blot images of Bax and β-actin 72hrs post-treatment with Pt II and Pt IV on A549 cells. ** indicates P<0.01 compared with the control. * indicates P<0.05 compared with the control (measured by one-way ANOVA). Data points denote mean ± SEM. n = 3 from three independent experiments.

3.6.3. B – cell Lymphoma 2 (Bcl2)

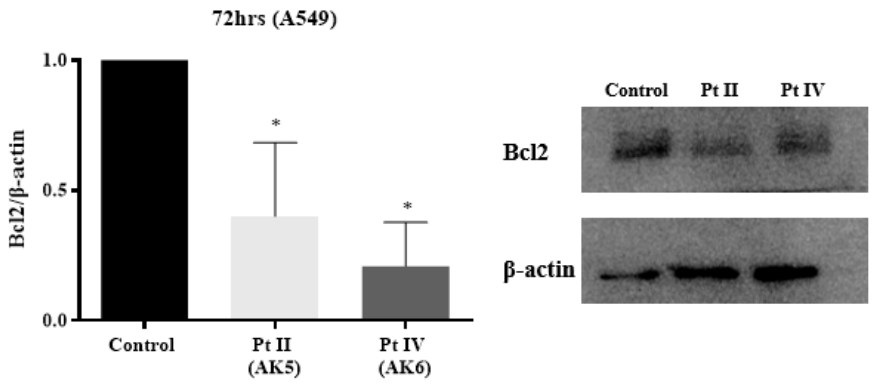

Figure 3.13: Bar graph and western blot images of Bcl2 and β-actin 72hrs post-treatment with Pt II and Pt IV on A549 cells. * indicates P<0.05 compared with the control (measured by one-way ANOVA). Data points denote mean ± SEM. n = 3 from three independent experiments.

3.6.4. BAX/Bcl2 Ratio

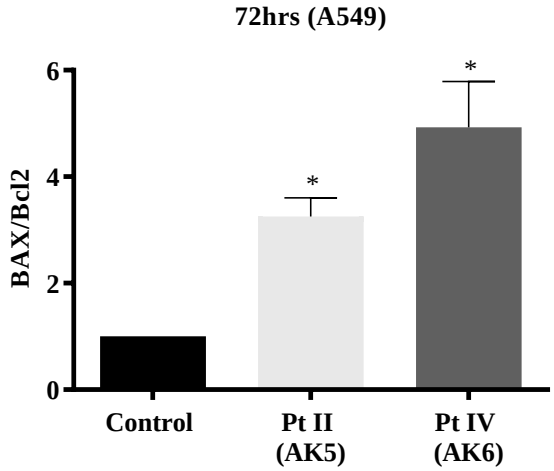

Figure 3.14: Bar graph representing Bax/Bcl2 72hrs post-treatment with Pt II and Pt IV on A549 cells. * indicates P<0.05 compared with the control (measured by one-way ANOVA). Data points denote mean ± SEM. n = 3 from three independent experiments.

3.6.5. Cytochrome c

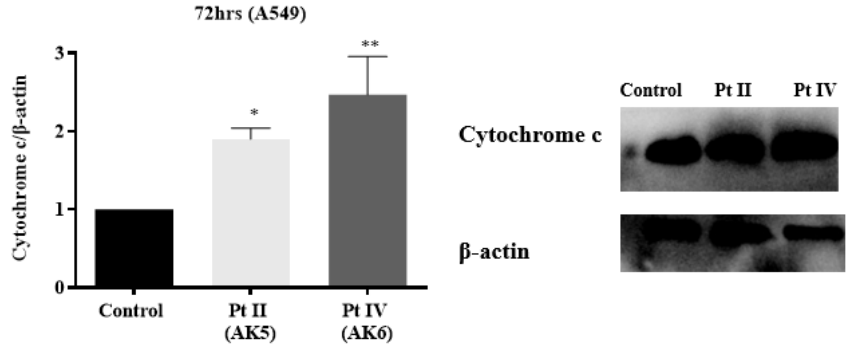

Figure 3.15: Bar graph representing Cytochrome c 72hrs post-treatment with Pt II and Pt IV on A549 cells. ** indicates P<0.01 compared with the control. * indicates P<0.05 compared with the control (measured by one-way ANOVA). Data points denote mean ± SEM. n = 3 from three independent experiments.

3.6.6. Cleaved Caspase 3

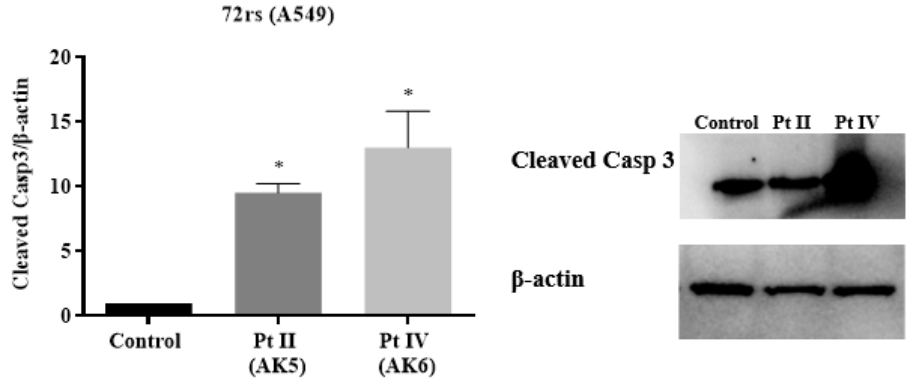

Figure 3.16: Bar graph representing Cleaved Caspase 3 72hrs post-treatment with Pt II and Pt IV on A549 cells. * indicates P<0.05 compared with the control (measured by one-way ANOVA). Data points denote mean ± SEM. n = 3 from three independent experiments.

3.7. Effect of Pt II and Pt IV complexes on DNA damage in A549 cells via the Comet Assay

The DNA damaging potential of the complexes Pt II and Pt IV was assessed using the alkaline comet assay. The A549 cells were treated for 72hrs with 4x the IC_{50} of each of the platinum complexes, and these results were compared with A549 cells treated with PBS or $KMnO_4$, which are negative and positive controls respectively. Multiple parameters were used to measure DNA damage and comet formation including head, tail and comet length and head, tail DNA content (table 3.3). To directly measure DNA damage, TMI was calculated by multiplying tail DNA content with tail length divided by 1000. Results show significant amounts of DNA damage in cells treated with the positive control and cells treated with Pt II and Pt IV when compared to the negative control (figure 3.19). Comet tails can be clearly identified in cells treated with $KMnO_4$ and the Pt II and Pt IV complexes (figures 3.17, 3.18).

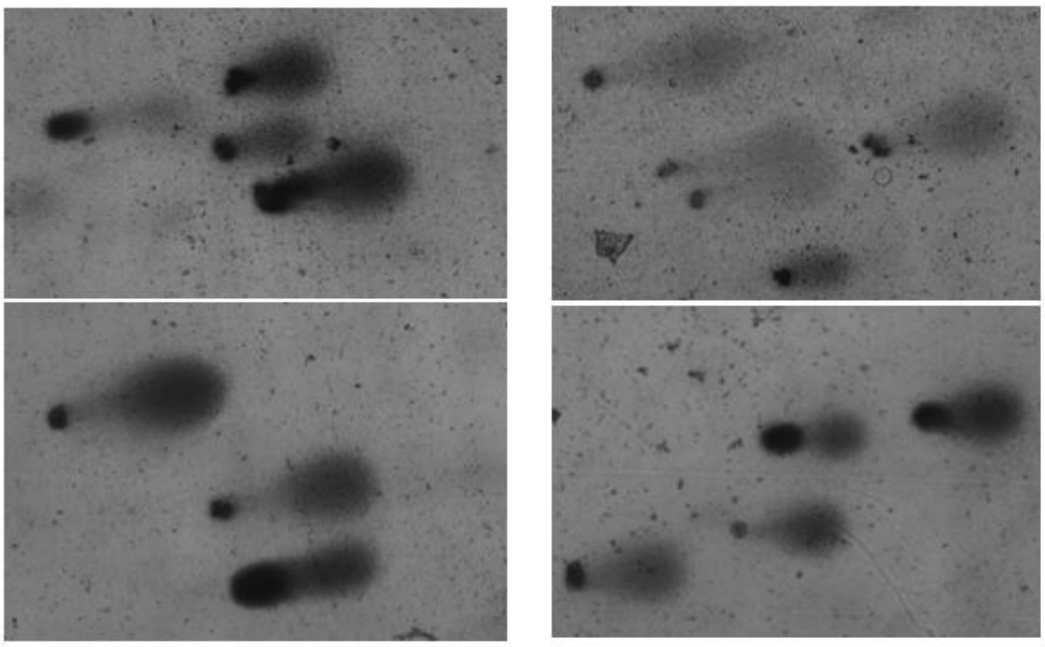

Figure 3.17: Microscopic images of comet formation when A549 cells were treated with Pt II and Pt IV. Images show the formation of comet 72hrs post – treatment with Pt II (left panel) and Pt IV complexes (right panel). Images taken at 100x magnification.

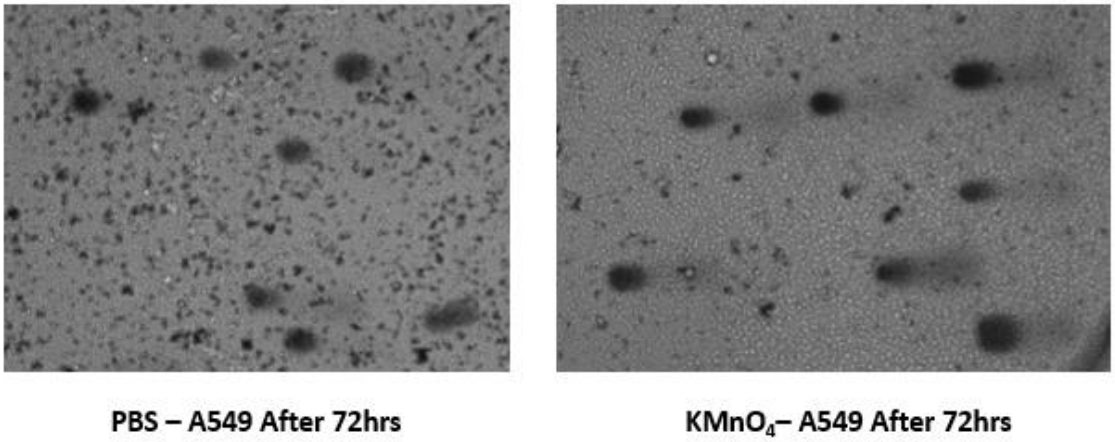

Figure 3.18: Microscopic images of comet formation when A549 cells were treated with PBS and $KMnO_4$. The negative control was treated with PBS and the positive control was treated with $KMnO_4$. All treatment conditions were over 72hrs. Images taken at 40x magnification.

Table 3.3: Effect on Pt II and Pt IV on DNA damage in A549 cells. DNA damage in A549 cells treated with Pt II and Pt IV for 72hrs. PBS and KMnO4 were respectively used as negative and positive controls. DNA damaged was assessed by the comet assay and parameters were measured by CASP (Comet assay software package). Data points denote mean ± SEM. n = 3 from three independent experiments where 50 images were taken at random.

	Negative Control (PBS)	**Positive Control ($KMnO_4$)**	**Pt II (AK5)**	**Pt IV (AK6)**
Head Length	220.22 ± 7.38	76.33 ± 16.58	68.22 ± 8.5	92.24 ± 9.29
Tail Length	32.94 ± 3.97	222 ± 52.58	209.67 ± 15.88	198.53 ± 9.25
Comet Length	253.17 ± 7.97	298.33 ± 66.46	277.9 ± 20.3	290.5 ± 12.71
Head DNA Content	95.79 ± 0.66	13.94 ± 6.85	7.91 ± 1.54	18.43 ± 2.57
Tail DNA Content	4.21 ± 0.7	86.06 ± 6.6	93.75 ± 0.92	81.58 ± 2.63
Tail Moment	1.7 ± 0.34	212.86 ± 58.42	189.71 ± 15.14	165.03 ± 9.76
Overall Tail Moment	4.85 ± 0.85	104.78 ± 66.27	66.29 ± 8.72	76.84 ± 6.68

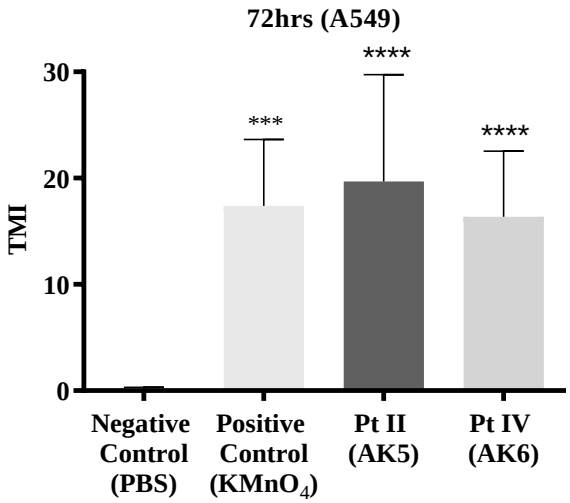

Figure 3.19: Tail Moment Index (TMI) as calculated from the comet assay data (n = 3). TMI = (Tail DNA Content x Tail Length) / 1000. **** indicates P<0.0001 compared with the control. *** indicates P<0.001 compared with the control. Data points denote mean ± SEM. n = 3 from three independent experiments where samples were run in duplicates.

Chapter Four

Discussion

Lung cancer is one of the deadliest types of cancer and it is therefore very important to find novel ways to improve the survival rates of patients (Siddiqui, et al., 2021). Cisplatin is a platinum II complex commonly used to treat a variety of cancer types including lung cancer; however, the search for other successful platinum complexes is still a need due to its general toxicity and significant side effects (Dasari & Tchounwou, 2014). In this study, the cytoxicity and the mode of action of novel Pt II and Pt IV complexes were investigated *in vitro* on the most common type of lung cancer using the NSCLC A549 cells (Zappa, et al., 2016). The cytotoxicity assay used the WST-1 reagent to measure viable cells upon treatment of A549 cells with different concentrations of Pt II and Pt IV for 72hrs (Scarcello et al., 2020). Results showed a dose-dependent A549 cell death with IC_{50} values in the sub-micromolar range for Pt II and low-micromolar range for Pt IV (figure 3.1, table 3.1), suggesting that both complexes have potent anti-neoplastic activity. Pt IV drugs were previously shown to overcome the toxicity problems commonly observed in Pt II drugs because the unique reducing environment produced by the cancer cells allows Pt IV complexes to selectively release the active form of the drug in hypoxic and low-pH environments (Li et al., 2019). In order to assess the selectivity of both complexes toward cancer cells, the cytotoxicity assay was also conducted on rat MSCs, which are considered close to normal cells. Surprisingly, both Pt II and Pt IV complexes exhibited very low

cytotoxicity against MSCs with 80% of the cells remained viable 72hrs post-treatment with the highest concentration used (figure 3.2). Such finding demonstrates the selective cytotoxicity of the complexes toward A549 cancer cells. Further *in vivo* studies in the future are required to confirm the observed *in vitro* selectivity.

Cellular uptake was also conducted on A549 cells using both complexes. The results indicate that the Pt II complex is being transported into A549 cells at a faster rate when comparing it to the Pt IV complex. This difference is attributed to the structure of these complexes, where Pt II complex is smaller and more hydrophobic than Pt IV, hence transported more easily across the A549 cells membrane (figure 1.3, figure 3.3). The uptake of Pt II and Pt IV complexes is time-dependent. The uptake may be mediated through passive transport, down a concentration gradient, or through active transport with the use of energy. The high intracellular to extracellular concentration observed in both Pt II and Pt IV complexes indicate that both complexes rely on active transported as a primary mean of uptake by A549 cells (table 3.2).

In order to assess the mode of cell death flow cytometry experiments were undertaken at different time points. This method requires the use of the phospholipid Phosphatidylserine (PS) as a marker of apoptosis (Demchenko, et al., 2013). The phospholipid bilayer of a viable cell is stabilized by an asymmetrical distribution of lipids, proteins and glycans; one important phospholipid is PS and it is located facing the cytosolic leaflet of the viable cell membrane (Demchenko, et al., 2013). During early and late apoptosis, PS is translocated and exposed to the outer leaflet to recruit phagocytes, initiate phagocytosis and terminate the apoptotic pathway. Annexin V is a stain that selectively binds to PS, with high affinity, when it is translocated onto the

outer leaflet of the apoptotic cell; therefore, both early and late apoptotic cells are stained with Annexin V (Demchenko, et al., 2013). Moreover, late apoptotic cells and necrotic cells completely lose their bilayer integrity and therefore both become permeable to the 7AAD stain that binds to DNA (Zimmermann, et al., 2011). The flow cytometry sorts the control and treated cells into four quadrants that reveal the percentages of viable cells (Annexin V and 7AAD negative), cells undergoing early apoptosis (Annexin V positive and 7AAD negative), late apoptosis (Annexin V positive and 7AAD positive) and necrosis (Annexin V negative and 7AAD positive). The results of the flow cytometry indicate that both platinum drugs are capable of inducing apoptotic cell death on the NSCLC cell line A549 starting at 24hrs post-treatment (figure 3.4, figure 3.7). Also, at 48hrs and 72hrs post-treatment, some of the A549 cells were necrotic (figure 3.5, 3.6, 3.8, 3.9). These results along with the cellular uptake results show that both Pt complexes reach high intracellular concentrations and are capable of inducing cell death mechanisms on the A549 cells starting 24hrs post-treatment.

Apoptosis is driven by intrinsic and extrinsic pathways each having specific proteins that can be quantified using western blots (Riss et al., 2021). The western blot experiment was conducted in order to look at apoptotic protein markers expression by A549 cells upon treatment with the Pt II or Pt IV complexes (Mahmood & Yang, 2012). All apoptotic markers tested were normalized over the levels of β-actin. The Bcl2-family of proteins consists of important regulators of the intrinsic pathway of apoptosis including pro-apoptotic protein Bax and the pro-survival protein Bcl2. Upon the induction of the intrinsic pathway of apoptosis, Bcl2 protein levels are

downregulated, releasing Bax and allowing its oligemerization on the mitochondrial membrane and thus making it permeable. Cytochrome c is another intrinsic apoptotic marker that is upregulated upon permeablization of the mitochondrial membrane (Renault et al., 2015). Treatment of A549 cells with the Pt II and Pt IV complexes showed significant upregulation in the protein levels of intrinsic apoptotic markers including the Bax/Bcl2 ratio and cytochrome c (figure 3.14, figure 3.15). The markers of the execution pathway are common for both the extrinsic and intrinsic pathways of apoptosis and they include caspase 3 which is activated indirectly by cytochrome c release and cleaved PARP which is activated by caspase 3 to finally induce apoptosis (Morales et al., 2014). Lung cancer cells treated with Pt II and Pt IV complexes have shown upregulated levels of cleaved caspase 3 and PARP which suggests the activation of the execution pathway through intrinsic intracellular signal transduction (figure 3.11, figure 3.16). Future experiments should be done to look at the protein levels of the extrinsic apoptotic markers like caspase 8. The results collectively confirm that the mode of action of both platinum complexes is via the intrinsic pathway of apoptosis.

Endogenous and exogenous agents, like reactive oxygen species and ultra violet (UV) light, trigger DNA damage that induces several responses in the human body including repair and cell death mechanisms (Norbury & Zhivotovsky, 2004). DNA damage can contribute to cancer progression by inducing mutations in cells that make them immortal and capable of indefinite replication (Basu et al., 2018). However, researchers have successfully manipulated the responses of the body to DNA damage to treat cancer, for example in radiotherapy and chemotherapy (Plesca et al., 2010).

The most successful chemotherapeutic in cancer treatment is the platinum II complex cisplatin and it is frequently used on lung cancer patients. Cisplatin enters the cancer cell via passive diffusion and binds to the DNA to induce DNA damage which will allow the cancer cells to activate cell repair or cell death pathways, primarily apoptosis (Rocha et al., 2018). To assess the production of reactive oxygen species by the Pt II and Pt IV complexes, A549 cells were treated and stained with DCFDA which transforms to the fluorescent agent DCF when the cells produce ROS (Wang & Roper, 2014). The tested platinum complexes both showed significant ROS production in A549 cancer cells 72hr post-treatment (figure 3.10). This suggests that ROS is the stimulus produced by Pt II and Pt IV to induce cell death by apoptosis. The comet assay was then used to look at various types of DNA damage by exposing the 549 cells *in vitro* to an electric current which moves the damaged DNA out of the nucleus forming a comet tail on the gel (Lu et al., 2017). The TMI or the tail moment index is calculated and it is important to assess the amounts of DNA damage in the A549 cells treated with Pt II, Pt IV in addition to A549 cells treated with PBS and potassium permanganate as a negative and positive controls respectively. The results in the images show visible comet tails which indicate DNA fragmentation by the Pt II and Pt IV complexes (figure 3.17, figure 3.18). The TMI calculated suggests significant DNA damage in A549 cells treated with the Pt II and Pt IV complexes (figure 3.19). Together, the flow cytometry, western blot, ROS assay and comet assay results, suggest that the mode of action of both Pt II and Pt IV complexes is through producing ROS which target the DNA to induce DNA damages that would activate cell death pathways in A549 cancer cells, primarily apoptosis (figure 4.1).

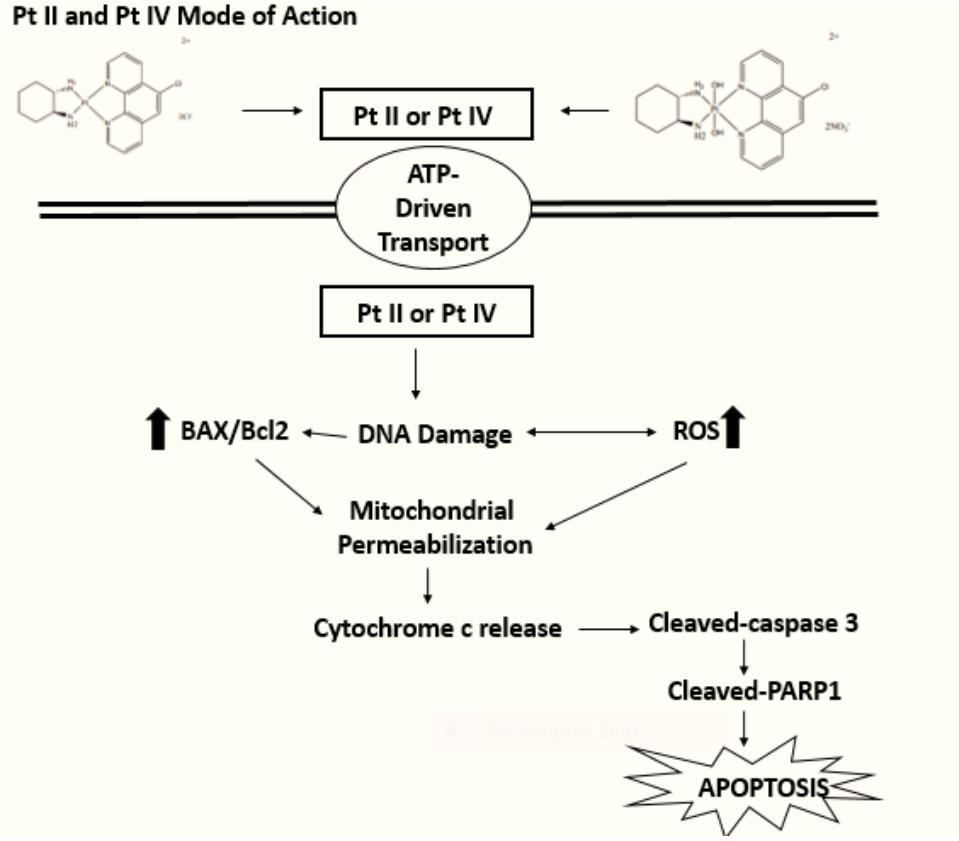

Figure 4.1: Pt II and Pt IV Mode of Action. Illustration showing that upon the uptake of the Pt complexes via active transport, the complexes trigger ROS overproduction and DNA damage to induce the activation of the intrinsic apoptotic pathway to kill the cancer cell.

Chapter Five

Conclusion

In conclusion, the two novel platinum complexes tested exhibited anti-neoplastic potentials toward A549 cancer cells. Pt II and Pt IV showed high cytotoxic activity and selectivity towards NSCLC cells. In addition, the active uptake of both complexes reached high intracellular concentrations and was time-dependent with Pt II being transported faster and at higher concentrations when compared to Pt IV. The mode of action of both complexes included free radical production, DNA damage and apoptosis. Future experiments would include testing the Pt II and Pt IV complexes on different cell lines to look at the potential effectiveness on different types of cancers including skin and breast cancer. Also, *in vivo* studies will be conducted on model organisms in order to confirm the selectivity and efficacy of the drugs in animal models. The significance of testing these novel anticancer platinum complexes is to mainly improve cancer treatment by finding novel chemotherapeutic agents that have better selectivity, efficacy and less side effects compared to currently existing chemotherapeutic drugs.

References

Alberts B, Johnson A, Lewis J, et al. (2002). Molecular Biology of the Cell. 4th edition. New York: Garland Science. Programmed Cell Death (Apoptosis) Available from: https://www.ncbi.nlm.nih.gov/books/NBK26873/

Anand, S. S., Singh, H., & Dash, A. K. (2009). Clinical Applications of PET and PET-CT. *Medical journal, Armed Forces India*, *65*(4), 353–358. https://doi.org/10.1016/S0377-1237(09)80099-3

Aykul, S., & Martinez-Hackert, E. (2016). Determination of half-maximal inhibitory concentration using biosensor-based protein interaction analysis. *Analytical biochemistry*, *508*, 97–103. https://doi.org/10.1016/j.ab.2016.06.025

Baik, J. Y., Liu, Z., Jiao, D., Kwon, H. J., Yan, J., Kadigamuwa, C., Choe, M., Lake, R., Kruhlak, M., Tandon, M., Cai, Z., Choksi, S., & Liu, Z. G. (2021). ZBP1 not RIPK1 mediates tumor necroptosis in breast cancer. *Nature communications*, *12*(1), 2666. https://doi.org/10.1038/s41467-021-23004-3

Baskar, R., Lee, K. A., Yeo, R., & Yeoh, K. W. (2012). Cancer and radiation therapy: current advances and future directions. *International journal of medical sciences*, *9*(3), 193–199. https://doi.org/10.7150/ijms.3635

Basu A. K. (2018). DNA Damage, Mutagenesis and Cancer. *International journal of molecular sciences*, *19*(4), 970. https://doi.org/10.3390/ijms19040970

Cafarotti, S., & Patella, M. (2020). Lung Cancer Surgical Management During the Outbreak of Coronavirus Disease 2019. *Journal of thoracic oncology : official publication of the International Association for the Study of Lung Cancer*, *15*(6), e81. https://doi.org/10.1016/j.jtho.2020.03.027

Cooper DB, McCathran CE. (2021). Cervical Dysplasia. *StatPearls Treasure Island: StatPearls Publishing*. https://www.ncbi.nlm.nih.gov/books/NBK430859/

Cooper GM. The Cell: A Molecular Approach. 2nd edition. Sunderland (MA): Sinauer Associates; 2000. The Development and Causes of Cancer. Available from: https://www.ncbi.nlm.nih.gov/books/NBK9963/

Dasari, S., & Tchounwou, P. B. (2014). Cisplatin in cancer therapy: molecular mechanisms of action. *European journal of pharmacology*, *740*, 364–378. https://doi.org/10.1016/j.ejphar.2014.07.025

Dela Cruz, C. S., Tanoue, L. T., & Matthay, R. A. (2011). Lung cancer: epidemiology, etiology, and prevention. *Clinics in chest medicine*, *32*(4), 605–644. https://doi.org/10.1016/j.ccm.2011.09.001

Demchenko A. P. (2013). Beyond annexin V: fluorescence response of cellular membranes to apoptosis. *Cytotechnology*, *65*(2), 157–172. https://doi.org/10.1007/s10616-012-9481-y

Dhuriya, Y. K., & Sharma, D. (2018). Necroptosis: a regulated inflammatory mode of cell death. *Journal of neuroinflammation*, *15*(1), 199. https://doi.org/10.1186/s12974-018-1235-0

Elmore S. (2007). Apoptosis: a review of programmed cell death. *Toxicologic pathology*, *35*(4), 495–516. https://doi.org/10.1080/01926230701320337

Fouad, Y. A., & Aanei, C. (2017). Revisiting the hallmarks of cancer. *American journal of cancer research*, *7*(5), 1016–1036.

Fritsch, M., Günther, S.D., Schwarzer, R. *et al.* Caspase-8 is the molecular switch for apoptosis, necroptosis and pyroptosis. *Nature* 575, 683–687 (2019). https://doi.org/10.1038/s41586-019-1770-6

Fulda, S., Debatin, KM. (2006) Extrinsic versus intrinsic apoptosis pathways in anticancer chemotherapy. *Oncogene* 25, 4798–4811. https://doi.org/10.1038/sj.onc.1209608

Garcia J, Hurwitz HI, Sandler AB, Miles D, Coleman RL, Deurloo R, Chinot OL. (2020). Bevacizumab (Avastin®) in cancer treatment: A review of 15 years of

clinical experience and future outlook. Cancer Treat Rev. doi: 10.1016/j.ctrv.2020.102017. Epub 2020 Mar 26. PMID: 32335505.

Glick, D., Barth, S., & Macleod, K. F. (2010). Autophagy: cellular and molecular mechanisms. *The Journal of pathology*, *221*(1), 3–12. https://doi.org/10.1002/path.2697

Gong, Y., Fan, Z., Luo, G., Yang, C., Huang, Q., Fan, K., Cheng, H., Jin, K., Ni, Q., Yu, X., & Liu, C. (2019). The role of necroptosis in cancer biology and therapy. *Molecular cancer*, *18*(1), 100. https://doi.org/10.1186/s12943-019-1029-8

Hanahan D, Weinberg RA. (2011). Hallmarks of cancer: the next generation. Cell. 4;144(5):646-74. doi: 10.1016/j.cell.2011.02.013

Hellmann, M. D., Chaft, J. E., William, W. N., Jr, Rusch, V., Pisters, K. M., Kalhor, N., Pataer, A., Travis, W. D., Swisher, S. G., Kris, M. G., & University of Texas MD Anderson Lung Cancer Collaborative Group (2014). Pathological response after neoadjuvant chemotherapy in resectable non-small-cell lung cancers: proposal for the use of major pathological response as a surrogate endpoint. *The Lancet. Oncology*, *15*(1), e42–e50. https://doi.org/10.1016/S1470-2045(13)70334-6

Hu, Z. G., Tian, Y. F., Li, W. X., & Zeng, F. J. (2019). Radiotherapy was associated with the lower incidence of metachronous second primary lung cancer. *Scientific reports*, *9*(1), 19283. https://doi.org/10.1038/s41598-019-55538-4

Huang Y, Lu Y, Vadlamudi M, Zhao S, Felmlee M, Rahimian R, Guo X. Intrapulmonary inoculation of multicellular spheroids to construct an orthotopic lung cancer xenograft model that mimics four clinical stages of non-small cell lung cancer. J Pharmacol Toxicol Methods. 2020 Jul-Aug;104:106885. doi: 10.1016/j.vascn.2020.106885. Epub 2020 Jun 10. PMID: 32531198.

Huang, C. Y., Ju, D. T., Chang, C. F., Muralidhar Reddy, P., & Velmurugan, B. K. (2017). A review on the effects of current chemotherapy drugs and natural agents in treating non-small cell lung cancer. *BioMedicine*, *7*(4), 23. https://doi.org/10.1051/bmdcn/2017070423

International B. R. (2020). Retracted: Apoptosis and Molecular Targeting Therapy in Cancer. *BioMed research international*, *2020*, 2451249. https://doi.org/10.1155/2020/2451249

Jan, R., & Chaudhry, G. E. (2019). Understanding Apoptosis and Apoptotic Pathways Targeted Cancer Therapeutics. *Advanced pharmaceutical bulletin*, *9*(2), 205–218. https://doi.org/10.15171/apb.2019.024

Khalid N, Azimpouran M. (2021). Necrosis. In: StatPearls [Internet]. Treasure Island (FL): StatPearls Publishing; Available from: https://www.ncbi.nlm.nih.gov/books/NBK557627/

Latimer KM, Mott TF. (2015). Lung cancer: diagnosis, treatment principles, and screening. Am Fam Physician. 15;91(4):250-6. PMID: 25955626.

Lemjabbar-Alaoui, H., Hassan, O. U., Yang, Y. W., & Buchanan, P. (2015). Lung cancer: Biology and treatment options. *Biochimica et biophysica acta*, *1856*(2), 189–210. https://doi.org/10.1016/j.bbcan.2015.08.002

Li, X., He, S., & Ma, B. (2020). Autophagy and autophagy-related proteins in cancer. *Molecular cancer*, *19*(1), 12. https://doi.org/10.1186/s12943-020-1138-4

Li, Y., An, L., Lin, J., Tian, Q., & Yang, S. (2019, July 24). Smart nanomedicine agents for cancer, triggered by pH, glutathione, H2: IJN. International Journal of Nanomedicine. https://doi.org/10.2147/IJN.S210116.

Lim, J. H., Oh, S., Kim, L., Suh, Y. J., Ha, Y. J., Kim, J. S., Kim, H. J., Park, M. H., Kim, Y. S., Cho, Y., Kwak, S. M., Lee, H. L., Kim, Y. S., & Ryu, J. S. (2021). Low-level expression of necroptosis factors indicates a poor prognosis of the squamous cell carcinoma subtype of non-small-cell lung cancer. *Translational lung cancer research*, *10*(3), 1221–1230. https://doi.org/10.21037/tlcr-20-1027

Lu, H. Y., Wang, X. J., & Mao, W. M. (2013). Targeted therapies in small cell lung cancer. *Oncology letters*, *5*(1), 3–11. https://doi.org/10.3892/ol.2012.791

Lu, Y., Liu, Y., & Yang, C. (2017). Evaluating In Vitro DNA Damage Using Comet Assay. *Journal of visualized experiments : JoVE*, (128), 56450. https://doi.org/10.3791/56450

Mahmood, T., & Yang, P. C. (2012). Western blot: technique, theory, and trouble shooting. *North American journal of medical sciences*, *4*(9), 429–434. https://doi.org/10.4103/1947-2714.100998

Mirsadraee, S., Oswal, D., Alizadeh, Y., Caulo, A., & van Beek, E., Jr (2012). The 7th lung cancer TNM classification and staging system: Review of the changes and implications. *World journal of radiology*, *4*(4), 128–134. https://doi.org/10.4329/wjr.v4.i4.128

Morales, J., Li, L., Fattah, F. J., Dong, Y., Bey, E. A., Patel, M., Gao, J., & Boothman, D. A. (2014). Review of poly (ADP-ribose) polymerase (PARP) mechanisms of action and rationale for targeting in cancer and other diseases. *Critical reviews in eukaryotic gene expression*, *24*(1), 15–28. https://doi.org/10.1615/critreveukaryotgeneexpr.2013006875

Nijkang, N. P., Anderson, L., Markham, R., & Manconi, F. (2019). Endometrial polyps: Pathogenesis, sequelae and treatment. *SAGE open medicine*, *7*, 2050312119848247. https://doi.org/10.1177/2050312119848247

Norbury, C., Zhivotovsky, B. DNA damage-induced apoptosis. *Oncogene* 23, 2797–2808 (2004). https://doi.org/10.1038/sj.onc.1207532

Pfeffer, C. M., & Singh, A. (2018). Apoptosis: A Target for Anticancer Therapy. *International journal of molecular sciences*, *19*(2), 448. https://doi.org/10.3390/ijms19020448

Plesca, D., Mazumder, S., & Almasan, A. (2008). DNA damage response and apoptosis. *Methods in enzymology*, *446*, 107–122. https://doi.org/10.1016/S0076-6879(08)01606-6

Power, S. P., Moloney, F., Twomey, M., James, K., O'Connor, O. J., & Maher, M. M. (2016). Computed tomography and patient risk: Facts, perceptions and uncertainties. *World journal of radiology*, *8*(12), 902–915. https://doi.org/10.4329/wjr.v8.i12.902

Purandare, N. C., & Rangarajan, V. (2015). Imaging of lung cancer: Implications on staging and management. *The Indian journal of radiology & imaging*, *25*(2), 109–120. https://doi.org/10.4103/0971-3026.155831

Qu, Y., Emoto, K., Eguchi, T., Aly, R. G., Zheng, H., Chaft, J. E., Tan, K. S., Jones, D. R., Kris, M. G., Adusumilli, P. S., & Travis, W. D. (2019). Pathologic Assessment After Neoadjuvant Chemotherapy for NSCLC: Importance and Implications of Distinguishing Adenocarcinoma From Squamous Cell Carcinoma. *Journal of thoracic oncology : official publication of the International Association for the Study of Lung Cancer*, *14*(3), 482–493. https://doi.org/10.1016/j.jtho.2018.11.017

Renault, T. T., Floros, K. V., Elkholi, R., Corrigan, K. A., Kushnareva, Y., Wieder, S. Y., Lindtner, C., Serasinghe, M. N., Asciolla, J. J., Buettner, C., Newmeyer, D. D., & Chipuk, J. E. (2015). Mitochondrial shape governs BAX-induced membrane permeabilization and apoptosis. *Molecular cell*, *57*(1), 69–82. https://doi.org/10.1016/j.molcel.2014.10.028

Rigden, H. M., Alias, A., Havelock, T., O'Donnell, R., Djukanovic, R., Davies, D. E., & Wilson, S. J. (2016). Squamous Metaplasia Is Increased in the Bronchial Epithelium of Smokers with Chronic Obstructive Pulmonary Disease. *PloS one*, *11*(5), e0156009. https://doi.org/10.1371/journal.pone.0156009

Riss TL, O'Brien MA, Moravec RA, et al. Apoptosis Marker Assays for HTS. 2021 Jul 1. In: Markossian S, Grossman A, Brimacombe K, et al., editors. Assay Guidance Manual [Internet]. Bethesda (MD): Eli Lilly & Company and the National Center for Advancing Translational Sciences; 2004-. Available from: https://www.ncbi.nlm.nih.gov/books/NBK572437/

Rivera, C., Gallegos, R., & Figueroa, C. (2020). Biomarkers of progression to oral cancer in patients with dysplasia: A systematic review. *Molecular and clinical oncology*, *13*(5), 42. https://doi.org/10.3892/mco.2020.2112

Rocha, C., Silva, M. M., Quinet, A., Cabral-Neto, J. B., & Menck, C. (2018). DNA repair pathways and cisplatin resistance: an intimate relationship. *Clinics (Sao Paulo, Brazil)*, *73*(suppl 1), e478s. https://doi.org/10.6061/clinics/2018/e478s

Rossi A, Di Maio M. (2016). Platinum-based chemotherapy in advanced non-small-cell lung cancer: optimal number of treatment cycles. Expert Rev Anticancer Ther. doi: 10.1586/14737140.2016.1170596. Epub 2016 A. PMID: 27010977.

Rudin, C. M., Brambilla, E., Faivre-Finn, C., & Sage, J. (2021). Small-cell lung cancer. *Nature reviews. Disease primers*, *7*(1), 3. https://doi.org/10.1038/s41572-020-00235-0

Salti, S. M., Hammelev, E. M., Grewal, J. L., Reddy, S. T., Zemple, S. J., Grossman, W. J., Grayson, M. H., & Verbsky, J. W. (2011). Granzyme B regulates antiviral CD8+ T cell responses. *Journal of immunology (Baltimore, Md. : 1950)*, *187*(12), 6301–6309. https://doi.org/10.4049/jimmunol.1100891

Sansregret, L., & Swanton, C. (2017). The Role of Aneuploidy in Cancer Evolution. *Cold Spring Harbor perspectives in medicine*, *7*(1), a028373. https://doi.org/10.1101/cshperspect.a028373

Scarcello, E., Lambremont, A., Vanbever, R., Jacques, P. J., & Lison, D. (2020). Mind your assays: Misleading cytotoxicity with the WST-1 assay in the presence of manganese. *PloS one*, *15*(4), e0231634. https://doi.org/10.1371/journal.pone.0231634

Siddiqui F, Siddiqui AH. Lung Cancer. (2021). In: StatPearls [Internet]. Treasure Island (FL): StatPearls Publishing; 2021 Jan-. Available from: https://www.ncbi.nlm.nih.gov/books/NBK482357/

Singh V, Sandean DP. CT Patient Safety And Care. (2021). *Treasure Island (FL): StatPearls Publishing*. https://www.ncbi.nlm.nih.gov/books/NBK567800/

Srinivas, U. S., Tan, B., Vellayappan, B. A., & Jeyasekharan, A. D. (2019). ROS and the DNA damage response in cancer. *Redox biology*, *25*, 101084. https://doi.org/10.1016/j.redox.2018.101084

Tan CP, Lu YY, Ji LN, Mao ZW. Metallomics insights into the programmed cell death induced by metal-based anticancer compounds. Metallomics. 2014 May;6(5):978-95. doi: 10.1039/c3mt00225j. PMID: 24668273.

Thandra, K. C., Barsouk, A., Saginala, K., Aluru, J. S., & Barsouk, A. (2021). Epidemiology of lung cancer. *Contemporary oncology (Poznan, Poland)*, *25*(1), 45–52. https://doi.org/10.5114/wo.2021.103829

Trivedi, S., Rosen, C. A., & Ferris, R. L. (2016). Current understanding of the tumor microenvironment of laryngeal dysplasia and progression to invasive cancer. *Current opinion in otolaryngology & head and neck surgery*, *24*(2), 121–127. https://doi.org/10.1097/MOO.0000000000000245

Turdo, A., Veschi, V., Gaggianesi, M., Chinnici, A., Bianca, P., Todaro, M., & Stassi, G. (2019). Meeting the Challenge of Targeting Cancer Stem Cells. *Frontiers in cell and developmental biology*, *7*, 16. https://doi.org/10.3389/fcell.2019.00016

Wallach, D., & Kovalenko, A. (2014). Keeping inflammation at bay. *eLife*, *3*, e02583. https://doi.org/10.7554/eLife.02583

Wang, X., & Roper, M. G. (2014). Measurement of DCF fluorescence as a measure of reactive oxygen species in murine islets of Langerhans. *Analytical methods : advancing methods and applications*, *6*(9), 3019–3024. https://doi.org/10.1039/C4AY00288A

Wang, Y., Qi, H., Liu, Y., Duan, C., Liu, X., Xia, T., Chen, D., Piao, H. L., & Liu, H. X. (2021). The double-edged roles of ROS in cancer prevention and therapy. *Theranostics*, *11*(10), 4839–4857. https://doi.org/10.7150/thno.56747

Xu, X., Lai, Y., & Hua, Z. C. (2019). Apoptosis and apoptotic body: disease message and therapeutic target potentials. *Bioscience reports*, *39*(1), BSR20180992. https://doi.org/10.1042/BSR20180992

Yang, H., Villani, R. M., Wang, H., Simpson, M. J., Roberts, M. S., Tang, M., & Liang, X. (2018). The role of cellular reactive oxygen species in cancer chemotherapy. *Journal of experimental & clinical cancer research : CR*, *37*(1), 266. https://doi.org/10.1186/s13046-018-0909-x

Yimit, A., Adebali, O., Sancar, A. *et al.* Differential damage and repair of DNA-adducts induced by anti-cancer drug cisplatin across mouse organs. *Nat Commun* 10, 309 (2019). https://doi.org/10.1038/s41467-019-08290-2

Yu, Z., Jiang, N., Su, W., & Zhuo, Y. (2021). Necroptosis: A Novel Pathway in Neuroinflammation. *Frontiers in pharmacology*, *12*, 701564. https://doi.org/10.3389/fphar.2021.701564

Yun, C. W., & Lee, S. H. (2018). The Roles of Autophagy in Cancer. *International journal of molecular sciences*, *19*(11), 3466. https://doi.org/10.3390/ijms19113466

Zappa, C., & Mousa, S. A. (2016). Non-small cell lung cancer: current treatment and future advances. *Translational lung cancer research*, *5*(3), 288–300. https://doi.org/10.21037/tlcr.2016.06.07

Zhang L, Hanigan MH. (2003). Role of cysteine S-conjugate beta-lyase in the metabolism of cisplatin. Journal of Pharmacology and Experimental Therapeutics. 306(3):988-94. doi: 10.1124/jpet.103.052225

Zhong Y, Jia C, Zhang X, Liao X, Yang B, Cong Y, Pu S, Gao C. Targeting drug delivery system for platinum(IV)-Based antitumor complexes. Eur J Med Chem. 2020 May 15;194:112229. doi: 10.1016/j.ejmech.2020.112229. Epub 2020 Mar 20. PMID: 32222677

Zimmermann M., Meyer N. (2011). Annexin V/7-AAD Staining in Keratinocytes. In: Stoddart M., editor. *Mammalian Cell Viability. Methods in Molecular Biology (Methods and Protocols)* Volume 740. Humana Press; New York, NY, USA: 2011. pp. 57–63.